




Inclusion of cGAMP within virus-like particle vaccines enhances their immunogenicity

Lise Chauveau^{1,†} , Anne Bridgeman^{1,†}, Tiong K Tan^{1,†}, Ryan Beveridge^{2,3}, Joe N Frost¹, Pramila Rijal¹, Isabela Pedroza-Pacheco⁴, Thomas Partridge⁴, Javier Gilbert-Jaramillo^{5,6}, Michael L Knight⁵, Xu Liu^{5,7}, Rebecca A Russell⁵, Persephone Borrow⁴ , Hal Drakesmith¹, Alain R Townsend¹ & Jan Rehwinkel^{1,*} 

Abstract

Cyclic GMP-AMP (cGAMP) is an immunostimulatory molecule produced by cGAS that activates STING. cGAMP is an adjuvant when administered alongside antigens. cGAMP is also incorporated into enveloped virus particles during budding. Here, we investigate whether inclusion of cGAMP within viral vaccine vectors enhances their immunogenicity. We immunise mice with virus-like particles (VLPs) containing HIV-1 Gag and the vesicular stomatitis virus envelope glycoprotein G (VSV-G). cGAMP loading of VLPs augments CD4 and CD8 T-cell responses. It also increases VLP- and VSV-G-specific antibody titres in a STING-dependent manner and enhances virus neutralisation, accompanied by increased numbers of T follicular helper cells. Vaccination with cGAMP-loaded VLPs containing haemagglutinin induces high titres of influenza A virus neutralising antibodies and confers protection upon virus challenge. This requires cGAMP inclusion within VLPs and is achieved at markedly reduced cGAMP doses. Similarly, cGAMP loading of VLPs containing the SARS-CoV-2 Spike protein enhances Spike-specific antibody titres. cGAMP-loaded VLPs are thus an attractive platform for vaccination.

Keywords cGAMP; influenza A virus; SARS-CoV-2; type I interferon; viral vaccine vector

Subject Categories Immunology; Methods & Resources; Microbiology, Virology & Host Pathogen Interaction

DOI 10.15252/embr.202152447 | Received 12 January 2021 | Revised 21 May 2021 | Accepted 26 May 2021 | Published online 18 June 2021

EMBO Reports (2021) 22: e52447

Introduction

Vaccination is a powerful strategy in the fight against infectious diseases, including virus infection. Indeed, vaccination led to the global eradication of smallpox and is highly protective against some viruses including measles virus and yellow fever virus. However, the development of vaccines inducing long-lasting and broadly effective protection has been difficult for other viruses such as human immunodeficiency virus (HIV) and influenza A virus (IAV), highlighting the need for new vaccination strategies (Rappuoli *et al*, 2011).

Successful vaccines induce potent adaptive immune responses. Vaccine-mediated protection against most virus infections is thought to be predominantly due to induction of antiviral antibody responses that prevent or rapidly control subsequent infection. Antibody responses limit virus infection and spread through several mechanisms (Pelegri *et al*, 2015). The most efficient one is mediated by neutralising antibodies that directly bind virus particles and prevent them from infecting cells. Following immunisation, antibodies are initially produced by short-lived extrafollicular plasmablasts. To achieve long-term protection, long-lived plasma cells and memory B cells must be generated in secondary lymphoid tissues. This process occurs in specialised structures called germinal centres (GCs) where B cells interact with multiple cell types that promote their maturation and differentiation into cells producing high-affinity antibodies that confer durable protection (Linterman & Hill, 2016; Cyster & Allen, 2019). CD4 T follicular helper (T_{fh}) cells are a CD4 T-cell subset specialised in providing help to B cells and are essential for GC formation. They increase the magnitude and quality of the humoral response by promoting B-cell proliferation, isotype switching and plasma cell differentiation; by mediating selection of high-affinity B cells in GCs; and by supporting the generation of

1 Medical Research Council Human Immunology Unit, Radcliffe Department of Medicine, Medical Research Council Weatherall Institute of Molecular Medicine, University of Oxford, Oxford, UK

2 MRC Molecular Hematology Unit, MRC Weatherall Institute of Molecular Medicine, John Radcliffe Hospital, University of Oxford, Oxford, UK

3 Virus Screening Facility, MRC Weatherall Institute of Molecular Medicine, John Radcliffe Hospital, University of Oxford, Oxford, UK

4 Nuffield Department of Clinical Medicine, University of Oxford, Oxford, UK

5 Sir William Dunn School of Pathology, University of Oxford, Oxford, UK

6 Department of Physiology, Anatomy and Genetics, University of Oxford, Oxford, UK

7 Key Laboratory of Human Disease Comparative Medicine, National Health Commission of China (NHC), Institute of Laboratory Animal Science, Peking Union Medicine College, Chinese Academy of Medical Sciences, Beijing, China

*Corresponding author. Tel: +44 1865 222 362; E-mail: jan.rehwinkel@imm.ox.ac.uk

†These authors contributed equally to this work

‡Present address: Institut de recherche en infectiologie de Montpellier (IRIM), CNRS UMR 9004, Montpellier, France

long-lived plasma cells and memory B cells (Crotty, 2019). In contrast, CD4 T follicular regulatory (Tfr) cells are involved in limiting GC reactions to prevent autoantibody formation. Therefore, the Tfh/Tfr ratio is important for regulation of GC responses (Sage *et al*, 2013).

Virus-specific cytotoxic T-cell (CTL) responses mediate clearance of infected cells to prevent virus spread and eradicate infection. If sterilising immunity is not conferred by antibodies, CTLs can make a key contribution to vaccine efficacy (Hansen *et al*, 2011). CTLs exert their activity by triggering destruction of infected cells via release of perforins and granzymes; by ligation of death-domain containing receptors and/or secretion of TNF α ; and by producing “curative” cytokines such as IFN γ . Both the magnitude, i.e. the number of activated cells, and polyfunctionality of the T-cell response, i.e. the capacity to mediate a breadth of effector activities including production of multiple cytokines, are important determinants of CD8 T-cell-based vaccine efficacy (Panagioti *et al*, 2018).

Initiation of virus-specific CD4 and CD8 T-cell responses requires presentation of viral antigens to naïve T cells by professional antigen-presenting cells (APCs), principally dendritic cells (DCs). T cells need to receive three signals for activation: T-cell receptor (TCR) triggering by contact with peptide-major histocompatibility complexes (MHC) (signal 1), costimulatory signals (signal 2) and inflammatory cytokines (signal 3) (Joffre *et al*, 2009).

Therefore, to induce adaptive immune responses, vaccines need to contain not only an appropriate antigen but also an adjuvant. Adjuvants exert a breath of effects; for example, they induce the expression of costimulatory molecules and cytokines by DCs (Coffman *et al*, 2010). There are only a limited number of FDA-approved adjuvants, most of which are based on aluminium salts (Shi *et al*, 2019). The increasing knowledge in the field of innate immunity, particularly in the mechanisms underlying pathogen recognition by innate immune receptors, provides an opportunity to develop new adjuvants that specifically engage such receptors and trigger a robust response (Temizoz *et al*, 2018). Adjuvants targeting Toll-like receptors or the cytosolic DNA sensing pathway have attracted a lot of attention (Dubensky *et al*, 2013). In particular, cyclic dinucleotides (CDNs), which activate stimulator of interferon genes (STING, also known as TMEM173, MPYS, ERIS and MITA) and induce a type I interferon (IFN-I) response as well as production of pro-inflammatory cytokines, are being developed as adjuvants (Cai *et al*, 2014). CDNs facilitate both CD8 T-cell and antibody responses (Li *et al*, 2013; Blaauboer *et al*, 2014; Kuse *et al*, 2019) and are effective as mucosal adjuvants (Ebensen *et al*, 2011; Blaauboer *et al*, 2015). 2'3' cyclic GMP-AMP (cGAMP) is of particular interest. It is produced by cGAMP synthase (cGAS) upon DNA sensing in the cell cytoplasm (Ablasser *et al*, 2013; Diner *et al*, 2013; Sun *et al*, 2013). Soluble cGAMP has been employed as an adjuvant in multiple pre-clinical vaccination models and is an anti-tumour agent (Li *et al*, 2013; Blaauboer *et al*, 2015; Corrales *et al*, 2015; Demaria *et al*, 2015; Temizoz *et al*, 2015; Lee *et al*, 2016; Li *et al*, 2016; Liu *et al*, 2016; Wang *et al*, 2016; Borriello *et al*, 2017; Takaki *et al*, 2017; Wang *et al*, 2017; Gutjahr *et al*, 2019; Luo *et al*, 2019; Vassilieva *et al*, 2019; Wang *et al*, 2020). However, soluble cGAMP levels are likely to diminish quickly in the extracellular milieu, due to diffusion from the site of administration and degradation by phosphodiesterases such as ectonucleotide pyrophosphatase/phosphodiesterase 1 (ENPP1), an enzyme degrading extracellular

ATP and cGAMP (Li *et al*, 2014; Carozza *et al*, 2020). Indeed, when injected intra-muscularly, the concentration of cGAMP at the inoculation site decreases rapidly, resulting in a sub-optimal adjuvant effect (Wang *et al*, 2016).

We and others previously showed that cGAMP is packaged into nascent viral particles as they bud from the membrane of an infected cell (Bridgeman *et al*, 2015; Gentili *et al*, 2015). Upon virus entry into newly infected cells, cGAMP is released into the cytosol and directly activates STING. Here, we took advantage of this observation and hypothesised that inclusion of the adjuvant cGAMP in viral vaccine vectors may enhance their immunogenicity by targeting adjuvant and antigen to the same cell and by protecting cGAMP from degradation in the extracellular environment. Indeed, using HIV-derived virus-like particles (VLPs), we found that the presence of cGAMP within VLPs enhanced adaptive immune responses to VLP antigens. Antigen-specific CD4 and CD8 T-cell responses were augmented, as well as neutralising antibody production. The latter was accompanied by an increase in Tfh cells in draining lymph nodes. The increased production of VLP-specific antibodies required STING. cGAMP-loaded VLPs containing the IAV haemagglutinin protein induced neutralising antibodies and conferred protection against development of severe disease after challenge with live IAV. Moreover, cGAMP-loaded VLPs provided protection at low doses, which is advantageous for vaccine production, and could improve safety. Finally, Spike-specific antibody titres were increased when we included cGAMP within VLPs containing the SARS-CoV-2 Spike protein, demonstrating the versatility of cGAMP-loaded VLPs for immunisation. Taken together, our proof-of concept study highlights the utility of cGAMP-loaded VLPs as a vaccine platform.

Results

cGAMP loading of HIV-derived VLPs

HIV-derived viral vectors and VLPs are routinely produced in the cell line HEK293T by transfection of plasmids encoding viral components (Milone & O'Doherty, 2018). Here, we generated VLPs by using plasmids expressing the HIV-1 capsid protein Gag fused to GFP (Gag-GFP) and the vesicular stomatitis virus envelope glycoprotein G (VSV-G). The resulting VLPs consist of a Gag-GFP core and a lipid membrane derived from the producer cell that is spiked with VSV-G proteins. Of note, these VLPs do not contain viral nucleic acid and can therefore not replicate in the host (Deml *et al*, 2005). Additional over-expression of cGAS in the VLP producer cells results in its activation, presumably by the transfected plasmid DNA, and in the presence of cGAMP in the cytosol. It is noteworthy that HEK293T cells do not express STING (Burdette *et al*, 2011); therefore, cGAS-overexpressing VLP producer cells do not respond to the presence of cGAMP. cGAMP is then packaged into the nascent viral particles, which are released as cGAMP-loaded VLPs (hereafter cGAMP-VLPs; Fig 1A). As a control, we produced VLPs that do not contain cGAMP (Empty-VLPs) by using a catalytically inactive version of cGAS.

To assess the efficiency of cGAMP incorporation into our VLPs, we extracted small molecules from VLPs as previously described (Mayer *et al*, 2017). cGAMP in the extract was then quantified by ELISA. While Empty-VLPs did not contain detectable levels of

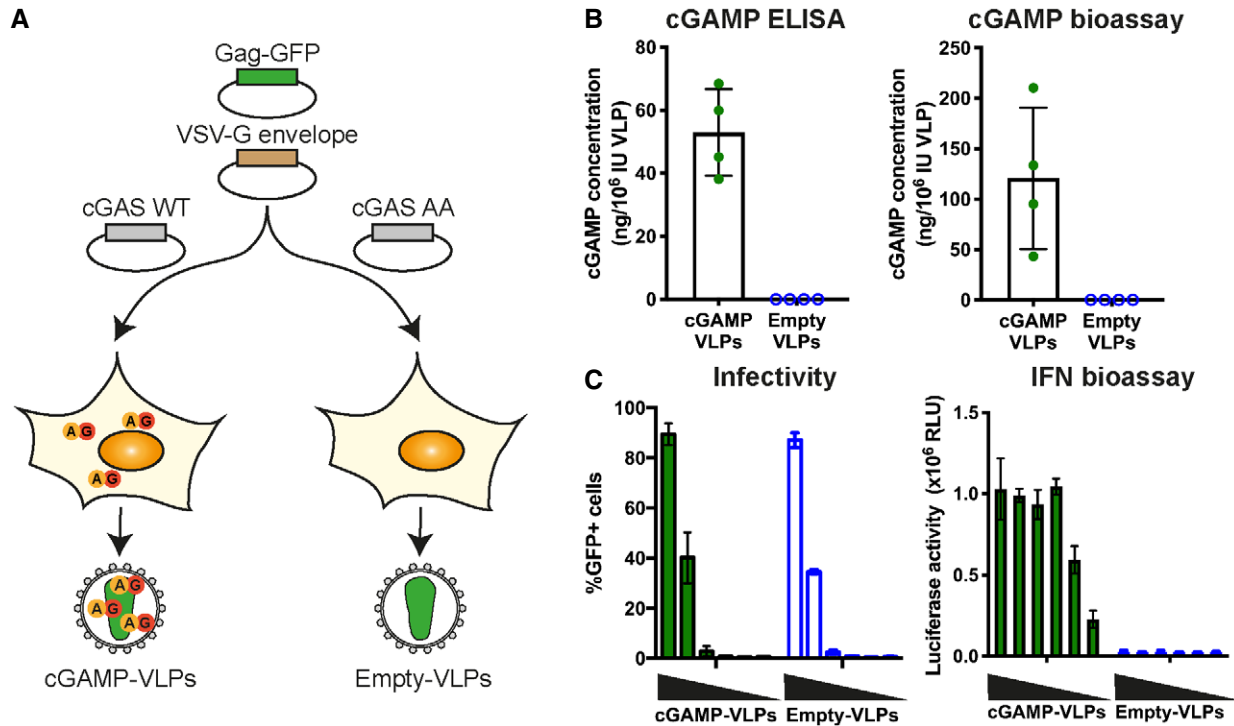


Figure 1. cGAMP incorporated into Gag-GFP virus-like particles (VLPs) induces IFN-I in infected cells.

A Schematic representation of cGAMP- and Empty-VLP production. HEK293T cells were transfected with plasmids encoding HIV-1 Gag-GFP and VSV-G envelope to enable VLP production. Overexpression of cGAS WT in the same cells generated cGAMP that was then incorporated into nascent VLPs (cGAMP-VLPs). As control, Empty-VLPs were produced in cells where a catalytically inactive cGAS (cGAS AA) was overexpressed.

B cGAMP is incorporated into cGAMP-VLPs. Small molecules were extracted from VLP preparations, and the cGAMP concentration was measured using a cGAMP ELISA and a cGAMP bioassay.

C cGAMP-VLPs induce an IFN-I response in target cells. HEK293 cells were infected with decreasing amounts of cGAMP-VLPs and Empty-VLPs (1/5 serial dilutions starting at 2 μ l of VLP stocks per well), and the infection was monitored 24 h later by quantifying GFP⁺ cells by flow cytometry. Supernatants from the same infected cells were then transferred to a reporter cell line expressing firefly luciferase under a promoter induced by IFN-I (ISRE). Luciferase activity measured 24 h later indicated the presence of IFN-I in the supernatants.

Data information: Data in (B) are pooled from four independent VLP productions. Each symbol corresponds to one VLP production, and mean and SD are shown. Data in (C) are pooled from three independent VLP productions tested simultaneously in infectivity and IFN-I bioassays; mean and SD are shown.

cGAMP, cGAMP-VLPs contained on average ~ 50 ng cGAMP per 10^6 infectious units (IU) of VLPs (Fig 1B). To confirm this result, we used a cGAMP bioassay in which semi-permeabilised THP-1 cells are stimulated with extracts from VLPs as described previously (Bridgeman *et al*, 2015). cGAMP levels determined by this assay were 2- to 3-fold higher compared with the ELISA data, with an average of ~ 120 ng cGAMP per 10^6 IUs (Fig 1B). These results were within the same range. The bioassay was likely less accurate as it involved stimulation of cells, and we therefore based further experiments on the ELISA results. Importantly, Empty-VLPs did not contain detectable levels of cGAMP measured by either method. cGAMP-VLPs and Empty-VLPs were equally infectious in HEK293 cells (Fig 1C). To confirm that cGAMP-VLPs trigger an IFN-I response, supernatant from the STING-positive HEK293 cells used in the infectivity assay was transferred to a reporter cell line expressing firefly luciferase under the interferon-sensitive response element (ISRE) promoter (Bridgeman *et al*, 2015). At similar infection rates, cGAMP-VLPs induced IFN-I production while Empty-VLPs did not (Fig 1C). Taken together, these results show that

cGAMP can be efficiently packaged into VLPs consisting of HIV-1 Gag-GFP and the VSV-G envelope.

Immunisation with cGAMP-VLPs induces higher and more polyfunctional CD4 and CD8 T-cell responses compared with Empty-VLPs

To test whether cGAMP-VLPs induce a better immune response than Empty-VLPs *in vivo*, we injected C57BL/6 mice intra-muscularly with 10^6 IU of cGAMP-VLPs or Empty-VLPs or, as a control, PBS. We first assessed CD4 T-cell responses in the spleen 14 days after immunisation. As we were unable to identify a specific peptide epitope within HIV-Gag recognised by CD4 T cells in H-2^b mice, we used bone marrow-derived myeloid cells (BMMCs) pulsed with cGAMP-VLPs for the evaluation of antigen-specific CD4 T-cell responses. We co-cultured these cells with splenocytes for 6 h before assessing IL2, IFN γ and TNF α production by CD4 T cells by intracellular cytokine staining (ICS). Compared to mice immunised with Empty-VLPs, we observed 2.7-fold increased frequencies of

CD4 T cells producing each of these cytokines in response to VLP-pulsed BMMCs in mice immunised with cGAMP-VLPs (Fig 2A and B). Moreover, cGAMP enhanced the proportion of cells that were able to co-produce two or all three cytokines (Fig 2C; 2.1- and 3.7-fold increases, respectively). Similar results were obtained when BMMCs were pulsed with Empty-VLPs (Fig EV1A and B).

We next assessed CD8 T-cell responses following immunisation. We screened a panel of overlapping 15-mer peptides spanning the HIV-1 Gag sequence and identified a peptide that stimulated an IFN γ response in cells from spleen in IFN γ ELISPOT assays (peptide p92; Fig EV1C and D). We then used NetMHCpan-3.0 (<http://www.cbs.dtu.dk/services/NetMHCpan-3.0/>; Nielsen & Andreatta, 2016) to predict the optimal epitope sequence recognised within p92 and identified a 9-mer peptide (SQVTNSATI, termed HIV-SQV) that triggered T-cell recognition more efficiently than the original 15-mer peptide (Fig EV1E and F). This 9-mer peptide was also reported to constitute an immunodominant HIV-1 Gag epitope in H-2^b mice in a prior study (Holechek *et al*, 2016). The HIV-SQV peptide was used for all subsequent analyses of VLP-elicited CD8 T-cell responses. We evaluated responses to the HIV-SQV peptide by IFN γ ELISPOT assay and showed that, when compared to Empty-VLPs, cGAMP-VLPs induced a modest but significant increase in the magnitude of the response (Fig 2D, 1.7-fold increase). To assess whether cGAMP loading of VLPs also enhanced the polyfunctionality of the responding CD8 T cells, we stimulated splenocytes for 6 h and stained for upregulation of CD107a (LAMP-1), a degranulation marker identifying cytotoxic cells, and for the production of IFN γ , TNF α and IL2 by ICS. Paralleling the results from the ELISPOT assay, CD8 T cells from mice immunised with cGAMP-VLPs showed a modest but significant increase in the frequency of cells upregulating CD107a (1.6-fold increase) and/or producing IFN γ (2-fold) and/or TNF α (1.9-fold) (Fig 2E and F). Furthermore, cGAMP enhanced the proportion of CD8 T cells that were able to co-produce two of the cytokines evaluated (Fig 2G; 1.9-fold increase).

Control of vaccinia virus infection by the immune system relies in part on CD8 T-cell responses (Xu *et al*, 2004). As immunisation with cGAMP-VLPs increased anti-HIV-Gag CD8 T-cell responses, we assessed whether this resulted in increased protection against subsequent infection with a vaccinia virus expressing the same HIV-Gag (vVK1 (Karacostas *et al*, 1989)). One month after immunisation, mice were challenged with vVK1, and 5 days after infection virus load in the ovaries was assessed by plaque assay. We observed no weight loss over the course of the infection (Fig EV2A). Immunisation with both VLPs reduced vVK1 load, and cGAMP-VLP-immunised mice showed a slight but non-significant increase in protection compared with animals immunised with Empty-VLPs (Fig EV2B and C).

Taken together, these results demonstrate that cGAMP loading of VLPs enhances polyfunctional CD4 and CD8 T-cell responses to VLP antigens.

cGAMP loading of VLPs enhances STING-dependent serum titres of VLP binding and neutralising antibodies

Next, we assessed the antibody response in immunised mice. We set up ELISAs that allow detection of serum antibodies binding to any protein in the VLPs (using lysates from cGAMP-VLPs for coating), or of antibodies specific for the VSV-G envelope or the

HIV-Gag protein. In mice immunised with VLPs, we detected very strong IgG responses and lower-titre IgM responses targeting VLP proteins 14 days after immunisation, indicating antibody class-switching (Figs 3A and EV3A). Interestingly, immunisation with cGAMP-VLPs induced stronger anti-VLP antibody responses compared with the Empty-VLP-immunised group, with statistically significant differences being observed in IgG2a/c and IgG2b levels. We also detected IgG antibodies targeting the VSV-G envelope, and IgG2a/c and IgG2b titres were significantly higher in the cGAMP-VLP-immunised group (Figs 3B and EV3A). Titres of antibodies recognising the intracellular antigen HIV-Gag were low or undetectable, but a similar trend was observed for a higher-magnitude response in the cGAMP-VLP-immunised group (Fig EV3B). Increased IgG2b anti-VLP antibody titres were also observed in cGAMP-VLP-immunised mice when sera were tested by ELISA using lysates from Empty-VLPs for coating (Fig EV3C).

We next tested whether the antibody response induced by cGAMP-VLPs was dependent on STING signalling. We immunised WT- or STING-deficient mice (*Tmem173*^{-/-}; hereafter referred to as *Sting*^{-/-} for simplicity) with VLPs and assessed the anti-VLP IgG2b response at day 14 after immunisation (Fig 3C). As a control for an adjuvant that does not depend on STING, we supplemented Empty-VLPs with 25 μ g poly(I:C), an immunostimulatory RNA that signals through Toll-like receptor 3 and RIG-I-like receptors (Empty-VLPs + poly(I:C)). In WT mice, immunisation with cGAMP-VLPs and Empty-VLPs + poly(I:C) each induced high titres of IgG2b antibodies that exceeded those elicited in the Empty-VLP group (Fig 3C). In *Sting*^{-/-} mice, immunisation with cGAMP-VLPs induced lower levels of IgG2b antibodies that were comparable with those in the Empty-VLP group, while the response to immunisation with Empty-VLPs + poly(I:C) remained unaffected (Fig 3C).

To test whether the anti-VLP antibodies were neutralising, we assessed the *in vitro* neutralisation capacity of sera using a VSV-G pseudotyped HIV-1-based lentivector expressing GFP (Fig 3D). The effect of pre-incubation with serum samples on the infectivity of the HIV-1-GFP virus was measured by monitoring GFP expression in HEK293 cells (Fig EV3D and E). Although immunisation with both cGAMP-VLPs and Empty-VLPs induced neutralising antibodies, this response was stronger when cGAMP was present within the VLPs, and sera from cGAMP-VLP immunised mice showed a 2.5 times higher half-maximal inhibitory concentration (Fig 3E and F).

In summary, immunisation with cGAMP-VLPs induced an increased antibody response that targeted proteins from total VLP lysates including the VSV-G envelope protein, and this anti-VLP response was dependent on STING signalling. Moreover, cGAMP loading enhanced production of virus neutralising antibodies.

Incorporation of cGAMP into VLPs increases the CD4 Tfh cell response

To gain insight into how immunisation with cGAMP-VLPs resulted in an increased antibody response, we investigated B- and T-cell populations in inguinal lymph nodes that drain the injection site. As CD4 T-cell responses were increased in the spleens of cGAMP-VLP-immunised mice, we first tested whether follicular CD4 T-cell numbers were elevated in lymphoid tissues draining the immunisation site. We identified follicular CD4 T cells as

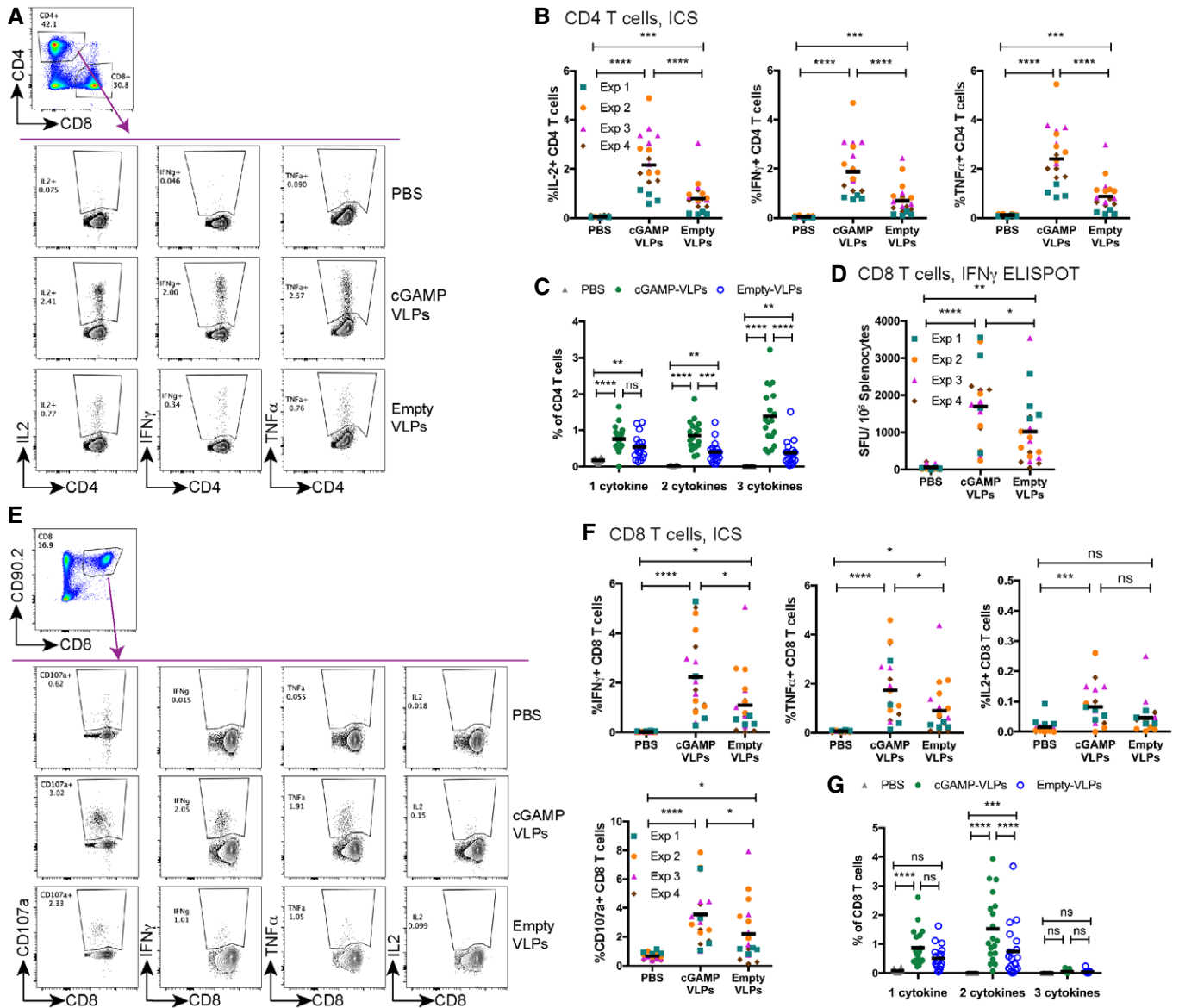


Figure 2. cGAMP loading of VLPs increases the magnitude of the CD4 and CD8 T-cell responses elicited after immunisation.

C57BL/6 mice were injected with cGAMP-VLPs, Empty-VLPs or PBS as a control *via* the intra-muscular route. 14 days later, VLP-specific T-cell responses were evaluated in the spleen.

A–C Immunisation with cGAMP-VLPs enhances VLP-specific CD4 T-cell responses. BMMCs from C57BL/6 mice were pulsed overnight with cGAMP-VLPs and used to stimulate cells from spleens of immunised mice. Cells were co-cultured for 6 h prior to evaluation of CD4 T-cell responses by ICS. CD4 T cells were gated as live, MHC-II⁺, CD4⁺, CD8[−]. CD4 T cells expressing IL2, IFN γ or TNF α were analysed as shown in (A). The percentage of total CD4 T cells producing each cytokine is shown in (B), and the percentage of CD4 T cells co-producing 1, 2 or 3 cytokines is shown in (C).

D–G Immunisation with cGAMP-VLPs facilitates induction of HIV-1 Gag-specific polyfunctional CD8 T-cell responses. Cells from spleens of immunised mice were stimulated with the HIV-SQV peptide. IFN γ -producing cells were enumerated by ELISPOT 24 h after stimulation with peptide (D). Alternatively, cells were analysed by ICS 6 h after stimulation with peptide. CD8 T cells were gated as live, CD90.2⁺, CD8⁺. CD8 T cells expressing CD107a, IFN γ , TNF α or IL2 were analysed as shown in (E). Panel F shows the percentage of total CD8 T cells upregulating CD107a and/or producing each cytokine, and panel G shows the percentage of CD8 T cells co-producing 1, 2 or 3 cytokines.

Data information: Panels (A) and (E) show representative examples of data from four independent experiments. In panels (B–D), (F) and (G), data are pooled from four independent experiments. A total of 19 mice was analysed per condition. Symbols show data from individual animals, and in (B), (D) and (F) are colour-coded by experiment. Horizontal lines indicate the mean. Statistical analyses were performed using a 2-way ANOVA followed by Tukey's multiple comparisons test. In (B), (D) and (F) data were blocked on experiments. ns $P \geq 0.05$; * $P < 0.05$; ** $P < 0.01$; *** $P < 0.001$; **** $P < 0.0001$. See also Figs EV1 and EV2.

CD4⁺CD44^{hi}PD1^{hi}CXCR5^{hi} and subdivided them into Tfh and Tfr cells by analysing FoxP3, which is expressed in Tfr cells (Fig 4A). Immunisation with VLPs led to an increase in the proportion of

follicular T cells within the CD4 T-cell population in the draining lymph node (Fig 4A and B). This was due to an expansion of Tfh cells, as the latter increased significantly in frequency after VLP

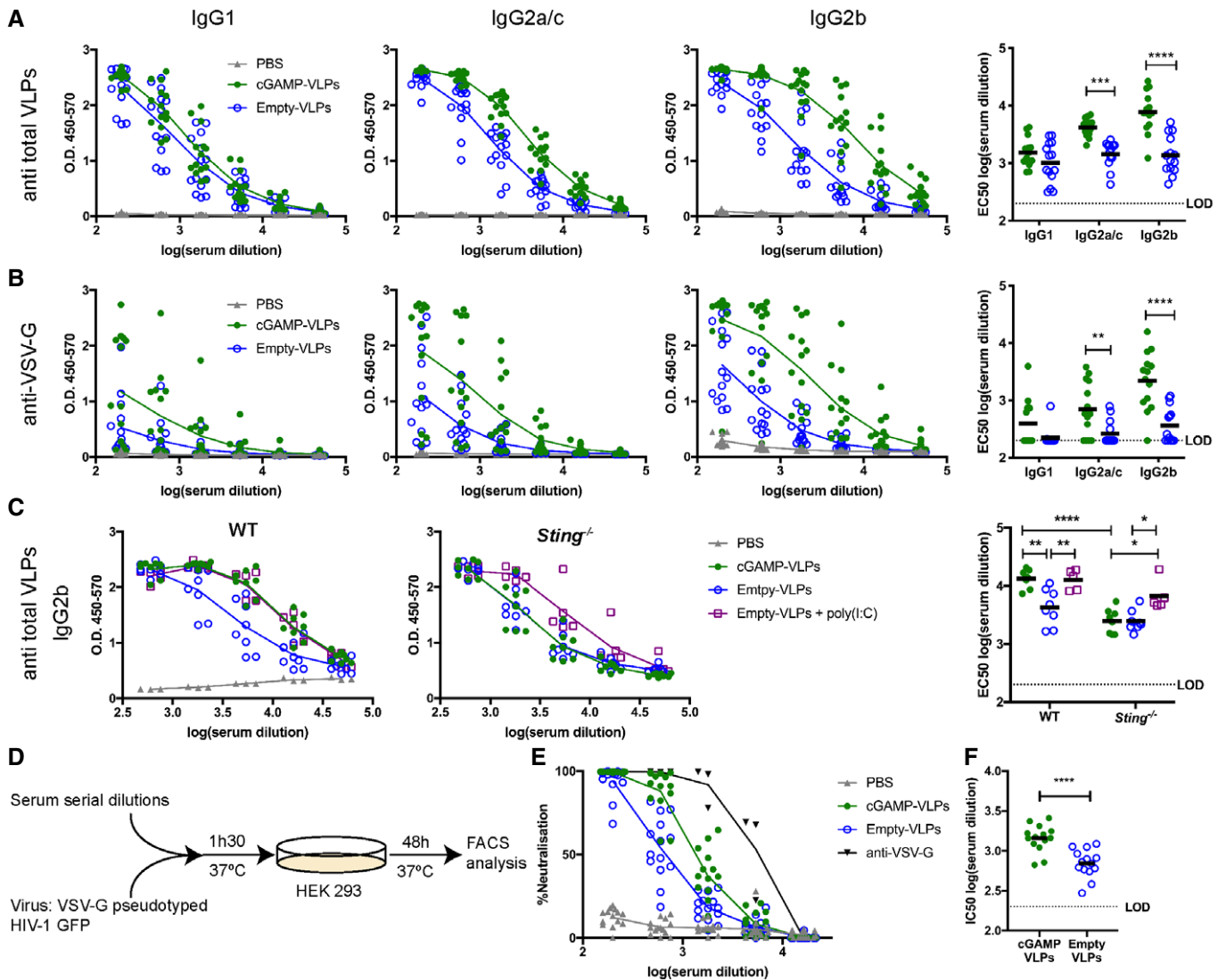


Figure 3. Immunisation with VLPs containing cGAMP increases neutralising antibody responses.

C57BL/6 mice were injected with cGAMP-VLPs, Empty-VLPs or PBS as a control *via* the intra-muscular route. Serum antibody responses were evaluated 14 days later. A, B cGAMP loading enhances IgG responses specific to VLP proteins, including VSV-G. ELISA plates were coated with lysate from cGAMP-VLPs (A) or recombinant VSV-G protein (B). Antibodies of different isotypes specific for these proteins were measured in sera from immunised mice by ELISA. The optical density at increasing serum dilutions is shown in the first three graphs from the left, and the EC50 is on the right. C Enhanced antibody production following immunisation with cGAMP-VLPs relies on STING signalling. WT or *Sting*^{-/-} mice were immunised with PBS, cGAMP-VLPs, Empty-VLPs or Empty-VLPs + poly(I:C). IgG2b antibodies recognising VLP proteins were assessed by ELISA. The optical density at increasing serum dilutions is shown in the first two graphs from the left, and the EC50 is on the right. D–F Immunisation with cGAMP-VLPs enhances production of neutralising antibodies. Serial dilutions of serum samples from individual mice were incubated with VSV-G pseudotyped HIV-1-GFP for 90 min at 37°C before infection of HEK293 cells. As a control, serial dilutions of the anti-VSV-G neutralising antibody 8G5F11 were tested in parallel. After 2 days, infection was measured by quantifying GFP⁺ cells by flow cytometry (D). Neutralising capacities of serum samples from individual animals were calculated as a percentage of neutralisation (calculated relative to the maximum infection in each experiment) (E) and as the half-maximal inhibitory concentration (IC50) (F).

Data information: In (A, B, E and F), data are pooled from three independent experiments and a total of 14 mice was analysed per condition. In (C), data are pooled from two independent experiments and 5–8 mice were analysed per condition. Symbols show data from individual animals, and the means are indicated. Statistical analyses were done using a 2-way ANOVA followed by Tukey's multiple comparisons test (A–C) or a Kruskal–Wallis test followed by Dunn's multiple comparisons test (F). ns $P \geq 0.05$; * $P < 0.05$; ** $P < 0.01$; *** $P < 0.001$; **** $P < 0.0001$. See also Fig EV3.

immunisation, whereas Tfr frequencies within CD4 T cells remained unaltered. As a consequence of this, there was a profound shift in the Tfh:Tfr ratio in VLP immunised as compared to control mice (Fig 4C). Importantly, the increase in Tfh cells was more

pronounced in cGAMP-VLP-immunised mice compared with Empty-VLP-injected animals (Fig 4B and C; 1.6-fold increase).

To assess the impact of this increased Tfh response on B-cell responses, we first gated on GC B cells (B220⁺IgD⁻CD95⁺GL7⁺ cells;

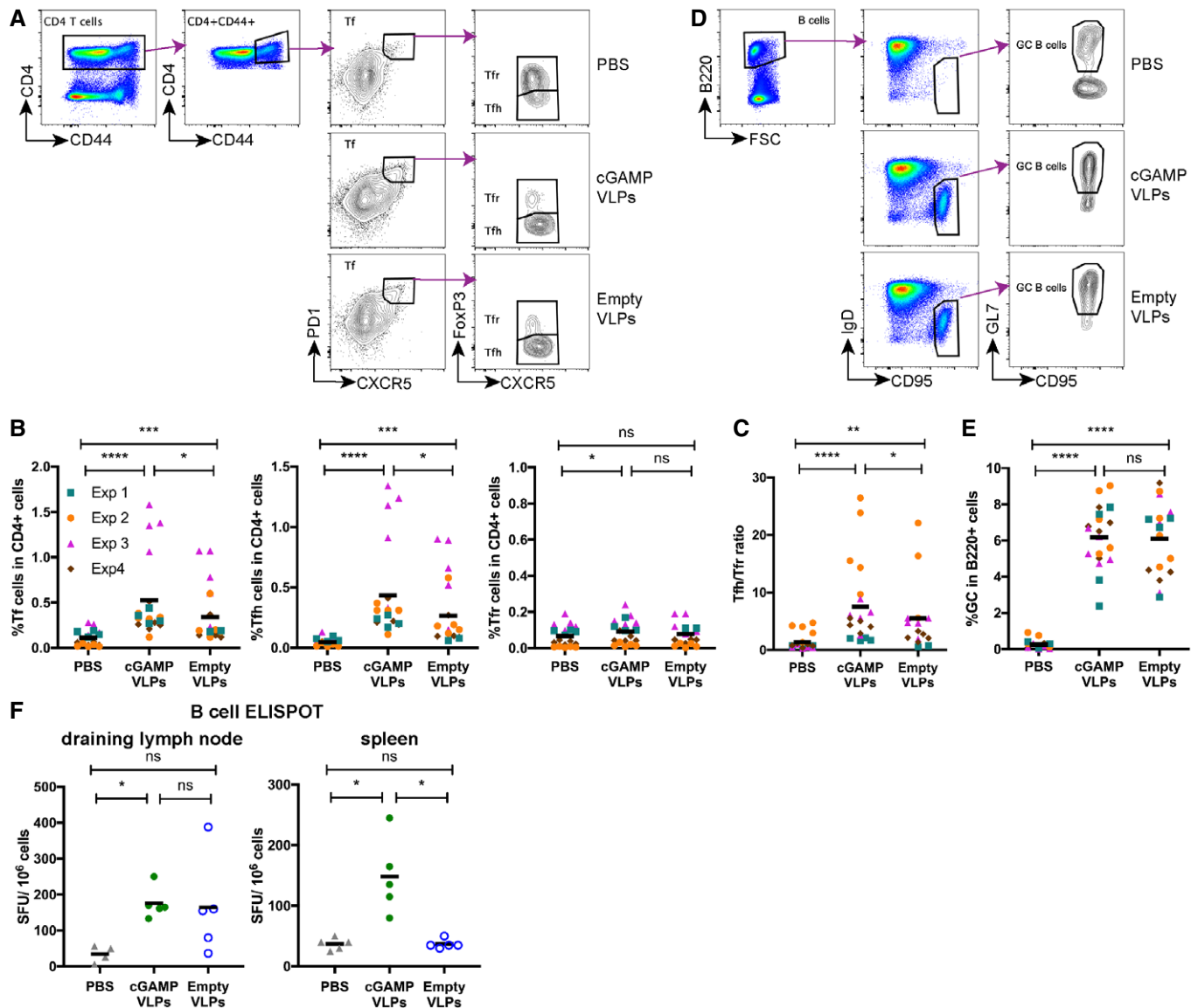


Figure 4. cGAMP loading of VLPs enhances induction of CD4 Tfh responses.

C57BL/6 mice were injected with cGAMP-VLPs, Empty-VLPs or PBS as a control *via* the intra-muscular route. 14 days later, T and B cells in the draining inguinal lymph nodes were characterised by flow cytometry and B-cell ELISPOT assays.

A–C Immunisation with cGAMP-VLPs enhances accumulation of Tfh cells in the draining lymph node. T follicular (Tf) cells were identified by flow cytometry as CD4⁺CD44⁺CXCR5^{hi}PD1^{hi} cells and were further subdivided into Tf cells (FoxP3⁺) and Tfr cells (FoxP3⁻). The gating strategy is shown in (A), and the percentages of Tf, Tfh and Tfr cells within CD4⁺ cells are shown in (B). The ratio of Tfh/Tfr is shown in (C).

D, E Immunisation with VLPs induces germinal centre formation. Germinal centre B cells were identified by flow cytometry as B220⁺IgD⁻CD95⁺GL7⁺ cells. The gating strategy is shown in (D), and the percentage of germinal centre B cells amongst B220⁺ cells is shown in (E).

F Immunisation with cGAMP-VLPs increases production of antibody-secreting cells. Cells from draining lymph nodes and spleens were seeded in ELISPOT plates coated with cGAMP-VLP lysates. After overnight incubation, cells producing VLP-specific IgG antibodies were identified using an anti-IgG Fc antibody.

Data information: Panels (A) and (D) show representative examples of data from four independent experiments. In (B), (C) and (E), data were pooled from four independent experiments including a total of 19 mice analysed per condition. Symbols show data from individual animals and are colour-coded by experiment. In (F), symbols show data from 5 mice per group measured in duplicate in one experiment. Horizontal lines indicate the mean. Statistical analyses were done using a 2-way ANOVA followed by Tukey's multiple comparisons test (B, C, E) or a Kruskal–Wallis test followed by Dunn's multiple comparisons test (F). ns $P \geq 0.05$; * $P < 0.05$; ** $P < 0.01$; *** $P < 0.001$; **** $P < 0.0001$.

Fig 4D). Immunisation with VLPs induced a robust GC B-cell response, with no difference being observed in the frequencies of GC B cells in cGAMP-VLP and Empty-VLP groups at the day 14 time-point analysed (Fig 4E). We next evaluated the generation of

antibody-secreting cells (ASCs) by antigen-specific B-cell ELISPOT assay on cells from both draining lymph nodes and spleens 14 days after immunisation. VLP-specific ASCs were detected in the lymph nodes of mice injected with both cGAMP-VLPs and Empty-VLPs

(Fig 4F). In the spleen, VLP-specific ASCs were also observed in cGAMP-VLP-immunised animals, but not in Empty-VLP-immunised animals (Fig 4F).

Taken together, these results suggest that immunisation with cGAMP-VLPs increased the antibody response by enhancing the accumulation of Tfh cells in draining lymph nodes, thereby promoting the development of ASCs.

cGAMP-VLPs pseudotyped with IAV haemagglutinin induce a neutralising antibody response and confer protection following live virus challenge

As immunisation with cGAMP-VLPs induced high titres of neutralising antibodies, we explored whether they could confer protection following a live virus challenge. Protection against IAV infection correlates with serum antibodies that have haemagglutination inhibition activity (Krammer, 2019). We therefore produced cGAMP-VLPs and Empty-VLPs incorporating the IAV surface glycoprotein haemagglutinin (HA) from the mouse-adapted PR8 strain of IAV (designated cGAMP-HA-VLPs and Empty-HA-VLPs, respectively) (Fig EV4A). cGAMP-HA-VLPs and Empty-HA-VLPs were equally infective, as assessed by the percentage of GFP-positive cells observed following infection of HEK293 cells with titrated doses of VLPs (Fig EV4B). Staining of infected HEK293 cells with the 21-D8-5A monoclonal antibody recognising HA revealed the presence of similar percentages of HA⁺ cells after infection with cGAMP-HA-VLPs and Empty-HA-VLPs (Fig EV4B). As control, cells infected with cGAMP-VLPs without HA showed no detectable staining. These data confirmed that HA was transferred by HA-VLPs to infected cells. Finally, we verified that supernatant from cells infected with cGAMP-HA-VLPs contained IFN-I, suggesting that the presence of HA did not affect the incorporation of cGAMP into the VLPs (Fig EV4C).

Next, we immunised mice with HA-VLPs. Two and 3 weeks after immunisation, sera were analysed for neutralising antibodies using a microneutralisation assay. In brief, a single cycle IAV expressing eGFP and PR8 HA was pre-incubated with sera and its infectivity was then monitored using MDCK-SIAT1 cells (Powell *et al*, 2012). Immunisation with both Empty-HA-VLPs and cGAMP-HA-VLPs induced neutralising antibodies, and the presence of cGAMP in the VLPs increased this response by 2.7-fold at week 2 and 2.5-fold at week 3 (Fig 5A and B). To determine whether immunisation conferred protection upon *in vivo* challenge with live IAV, we infected mice with 10⁴ TCID₅₀ (Median Tissue Culture Infectious Dose) of HA-matched PR8 IAV 1 month after immunisation. Animals immunised with 10⁶ infectious units of both VLPs were protected against the weight loss observed between days 3 and 4 after IAV infection in PBS-treated mice, both resulting in 100% survival (Fig 5C and D). This prompted us to reduce the amount of VLPs used for immunisation. At an intermediate dose of 2 × 10⁵ infectious units of VLPs, cGAMP-HA-VLPs induced a 2.4-fold higher antibody response at week 3 (Fig 5B) and were fully protective against weight loss and disease progression to an end-point where humane sacrifice was necessary, while immunisation with Empty-HA-VLPs only delayed disease progression by about 4 days, resulting in 100 and 16.7% survival, respectively (Fig 5C and D). At the lowest dose of VLPs tested (5 × 10⁴ infectious units), cGAMP-HA-VLPs induced a 3.6-fold higher antibody response at week 3

(Fig 5B). Empty-HA-VLPs were not protective whereas cGAMP-HA-VLPs protected most animals against severe disease (83% survival) (Fig 5C and D).

To compare our strategy of loading VLPs with cGAMP with an unrelated adjuvant as a benchmark, we supplemented Empty-HA-VLPs with AddaVax, a squalene-based oil-in-water emulsion similar to the adjuvant currently approved in Europe for the influenza vaccine (MF59) (Ott *et al*, 1995). We found that both cGAMP-HA-VLPs and Empty-HA-VLPs injected together with AddaVax conferred full protection against subsequent IAV challenge and induced similar neutralising antibody titres (Fig 6).

To test whether the protective effect of cGAMP-loaded VLPs required cGAMP to be present within VLPs, we compared cGAMP-HA-VLPs with Empty-HA-VLPs mixed prior to immunisation with chemically synthesised cGAMP. In these experiments, we used 5 × 10⁴ infectious units of cGAMP-HA-VLPs containing ~3.5 ng cGAMP (cGAMP content of cGAMP-HA-VLPs used was quantified by ELISA as in Fig 1B). We therefore administered either 3.5 ng or 35 ng cGAMP mixed with Empty-HA-VLPs (Empty-HA-VLPs + matched cGAMP or 10× cGAMP) to mice for comparison with cGAMP-HA-VLPs. One month after immunisation, mice were challenged with 10⁴ TCID₅₀ of HA-matched PR8 IAV. With the exception of a single animal receiving 10× cGAMP, Empty-HA-VLPs without or with added cGAMP failed to protect mice from weight loss whereas cGAMP-HA-VLPs were fully protective, as observed before (Fig 6A and B). These results were paralleled by serum neutralising antibody titres at week 3 (Fig 6C and D) and showed that, to exert a protective effect, cGAMP needed to be present within VLPs.

Taken together, these results show that vaccination with VLPs incorporating IAV HA induced neutralising antibodies in mice, which were protected against subsequent IAV challenge. Incorporation of cGAMP into HA-VLPs was as efficient as a benchmark adjuvant (AddaVax) in inducing protection against IAV. Moreover, the presence of cGAMP in HA-VLPs, but not exogenous cGAMP mixed with HA-VLPs, enhanced the neutralising antibody response and, particularly at lower doses of VLPs used for immunisation, facilitated protection against IAV.

cGAMP loading of VLPs containing the SARS-CoV-2 Spike protein augments antibody responses

Finally, we wished to explore the versatility of cGAMP-loaded VLPs as vaccine vectors by incorporating another viral antigen. Given the urgent need for vaccines against SARS-CoV-2, we produced VLPs in HEK293T cells expressing the SARS-CoV-2 Spike (S) protein, a viral envelope protein that contains key antigens recognised by neutralising antibodies (Zhou *et al*, 2020). S is processed by cellular proteases into S1 and S2 subunits that remain non-covalently associated at the surface of the viral particle (Hoffmann *et al*, 2020). Western blot analysis showed S2 was incorporated at comparable levels in cGAMP-S-VLPs and Empty-S-VLPs (Fig 7A). We collected serum samples 3 weeks after immunisation with cGAMP-S-VLPs and Empty-S-VLPs and analysed S-specific antibody titres using two different ELISA setups. The presence of cGAMP in VLPs enhanced the titres of antibodies recognising full-length S (Fig 7B) as well as its receptor-binding domain (RBD; Fig 7C), which interacts with the cellular receptor ACE2. We also determined the virus neutralisation

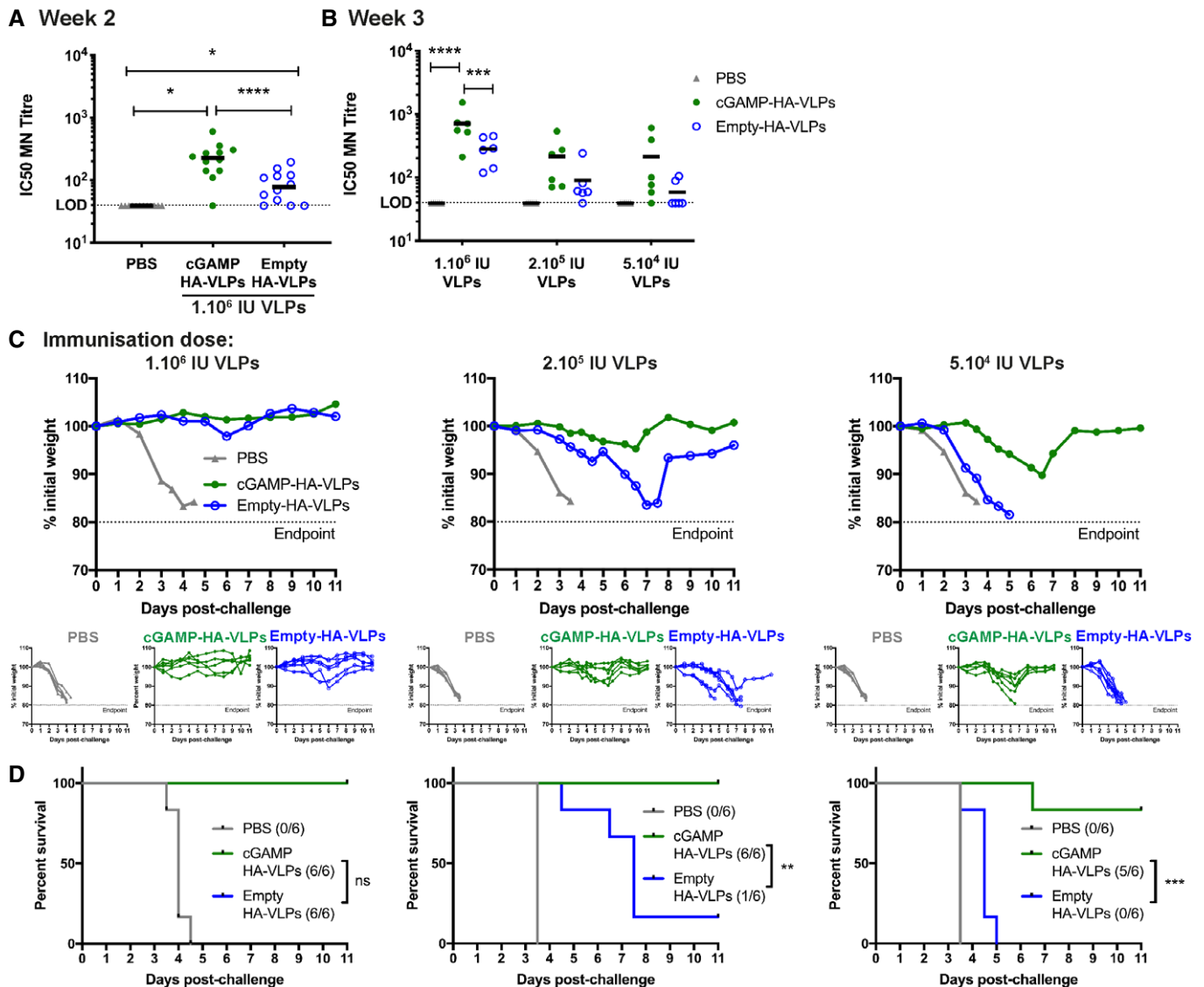


Figure 5. cGAMP-VLPs pseudotyped with IAV HA induce neutralising antibodies and confer protection following IAV infection.

C57BL/6 mice were immunised with PBS as a control, cGAMP-HA-VLPs or Empty-HA-VLPs *via* the intra-muscular route.

A, B VLPs pseudotyped with IAV HA induce neutralising antibodies. Two (A) or three (B) weeks after immunisation with the indicated doses of VLPs, sera were collected, heat-inactivated, and titres of antibodies capable of neutralising an IAV expressing a matched HA protein were determined by microneutralisation (MN) assay. The dotted line shows the limit of detection (LOD).

C, D Low doses of cGAMP-HA-VLPs confer protection following IAV challenge. One month after immunisation with the indicated doses of VLPs, animals were infected with 10^4 TCID₅₀ of IAV PR8 virus. Weight loss was monitored over the following 11 days and is shown as a percentage of starting weight (C, upper graph shows mean and lower graphs show individual mice for each condition). Animals approaching the humane end-point of 20% weight loss were culled and survival to end-point curves are shown in (D).

Data information: In (A), data were pooled from two independent experiments including a total of 12 mice per condition. In (B–D), 6 mice per group were analysed for each VLP dose. In (A) and (B), symbols show data from individual animals. Horizontal lines indicate the mean. Statistical analyses were done using a Kruskal–Wallis test followed by Dunn's multiple comparisons test (A), a 2-way ANOVA followed by Tukey's multiple comparisons test (B) or a survival analysis with the log-rank (Mantel–Cox) test (D). ns $P \geq 0.05$; * $P < 0.05$; ** $P < 0.01$; *** $P < 0.001$; **** $P < 0.0001$. See also Fig EV4.

capacity of antibodies induced after immunisation with VLPs containing S. We incubated live SARS-CoV-2 with serum samples and subsequently infected Vero cells. After overnight incubation, cells were fixed and stained with a nucleocapsid-specific antibody to reveal foci of infected cells (Fig EV5A). As a positive control, we used the RBD-specific and neutralising EY6A antibody (Zhou *et al*,

2020). As expected, EY6A reduced the number of infected foci (Fig EV5A and B). Similarly, sera from seven of twelve mice immunised with cGAMP-S-VLPs neutralised SARS-CoV-2 (Figs 7D and EV5A and B). In contrast, the serum from only four of twelve animals administered with Empty-S-VLPs reduced the infectivity of the virus, and samples from PBS-treated control mice had no effect. In

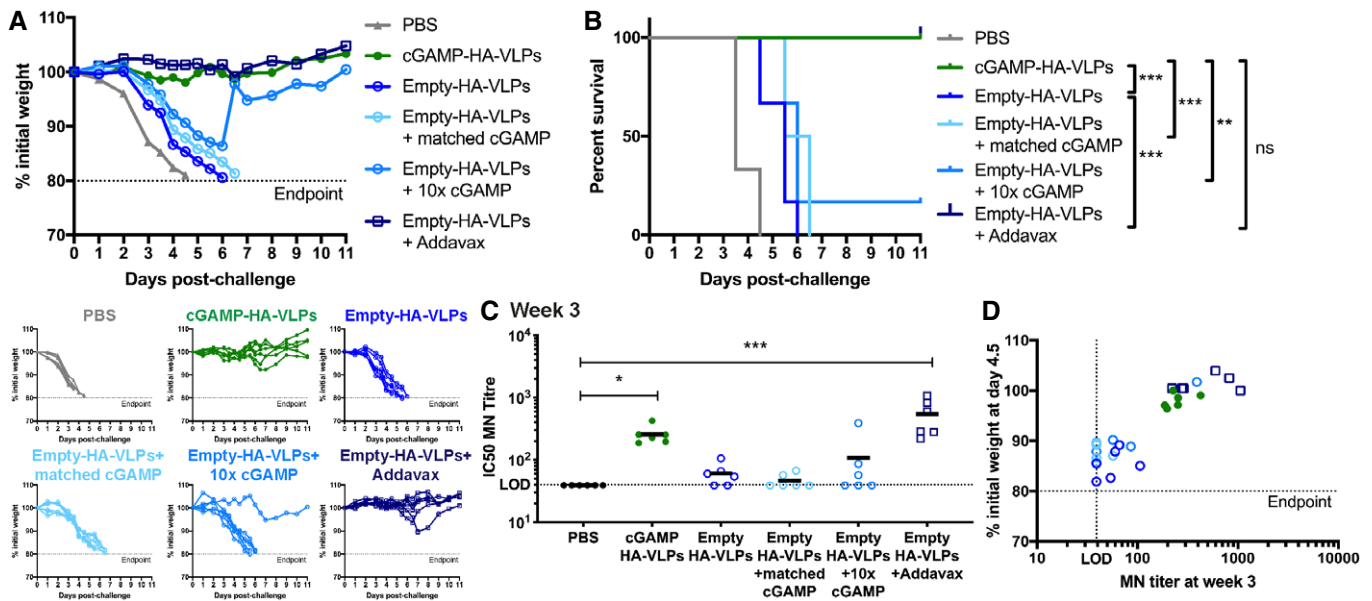


Figure 6. Incorporation of cGAMP within VLPs is essential for its protective effect.

Mice were immunised *via* the intra-muscular route with 5×10^4 IU of cGAMP-HA-VLPs, Empty-HA-VLPs, Empty-HA-VLPs + matched cGAMP (3.5ng), Empty-HA-VLPs + 10x cGAMP (35 ng), Empty-HA-VLPs + AddaVax (1:1 vol ratio) or PBS as a control.

A, B cGAMP-HA-VLPs and Empty-HA-VLPs + AddaVax protect against IAV challenge. One month after immunisation, animals were infected with 10^4 TCID₅₀ of IAV PR8 virus. Weight loss was monitored over the following 11 days and is shown as a percentage of starting weight (A, upper graph shows mean and lower graphs show individual mice for each condition). Animals approaching the humane end-point of 20% weight loss were culled and survival to end-point curves are shown in (B).

C, D cGAMP-HA-VLPs and Empty-HA-VLPs + AddaVax induce neutralising antibody responses that accompany protection. Three weeks after immunisation with 5×10^4 IU of the indicated HA-VLPs, sera were collected and heat-inactivated. Titres of antibodies capable of neutralising an IAV expressing a matched HA protein were determined by microneutralisation (MN) assay (C). The dotted line shows the limit of detection (LOD). Correlation between the MN titres at week 3 and the weight loss at day 4.5 post-challenge is shown in (D).

Data information: 6 mice per group were analysed for each HA-VLP and PBS. In (C) and (D), symbols show data from individual animals. In (C), horizontal lines indicate the mean. Statistical analyses were done using a survival analysis with the log-rank (Mantel–Cox) test (B) or a Kruskal–Wallis test followed by Dunn’s multiple comparisons test (C). ns $P \geq 0.05$; * $P < 0.05$; ** $P < 0.01$; *** $P < 0.001$.

sum, these observations suggest that cGAMP loading of VLPs enhances the titres of SARS-CoV-2 neutralising antibodies upon immunisation.

Discussion

New and/or more targeted adjuvants are needed for improved efficacy and safety of vaccines. There is growing interest in using adjuvants that specifically activate innate immune pathways used by cells to detect viral infections. cGAMP is one such example. cGAMP is a natural molecule produced by cells upon virus infection that specifically triggers STING, thereby inducing innate and adaptive immune responses. The vaccination strategy we describe here is based on coupling the adjuvant cGAMP with antigen(s) in a single entity, namely HIV-derived VLPs. We demonstrate that cGAMP loading of these VLPs increased CD4 and CD8 T-cell responses, as well as antibody responses, against protein antigens in the VLPs. As expected, the enhanced antibody response in mice immunised with cGAMP-VLPs was dependent on the expression of STING. Furthermore, vaccination with VLPs containing cGAMP protected mice against disease development following infection with a virus expressing a cognate antigen.

2′3′-cGAMP has attracted a lot of interest as an adjuvant since its identification in 2013 (Ablasser *et al*, 2013; Diner *et al*, 2013; Gao *et al*, 2013; Wu *et al*, 2013; Zhang *et al*, 2013). It is the CDN that is best recognised by all human STING variants, making it an ideal candidate adjuvant (Yi *et al*, 2013; Corrales *et al*, 2015). 2′3′-cGAMP has been tested pre-clinically in prophylactic vaccination models against infectious diseases and tumours, and as a therapeutic compound against tumours (Li *et al*, 2013; Blaauboer *et al*, 2015; Demaria *et al*, 2015; Temizoz *et al*, 2015; Lee *et al*, 2016; Li *et al*, 2016; Liu *et al*, 2016; Wang *et al*, 2016; Borriello *et al*, 2017; Takaki *et al*, 2017; Wang *et al*, 2017; Gutjahr *et al*, 2019; Luo *et al*, 2019; Vassilieva *et al*, 2019; Wang *et al*, 2020). These studies employed different vaccine formulations and delivery routes, ranging from co-injection with protein antigens or with inactivated virus to incorporation into nanoparticles that mimic pulmonary surfactant. In these reports, doses typically ranged from 1 to 20 µg per mouse. In contrast, we show here that incorporating cGAMP into VLPs was efficacious at doses as low as 3.5ng per mouse. An equivalent dose—or even a ten times excess—of soluble cGAMP co-injected with Empty-VLPs neither induced a neutralising antibody response to IAV nor protected against IAV challenge. cGAMP loading of VLPs therefore allows for a notable reduction in the dose of this adjuvant needed to induce protective immunity. Possible explanations for this

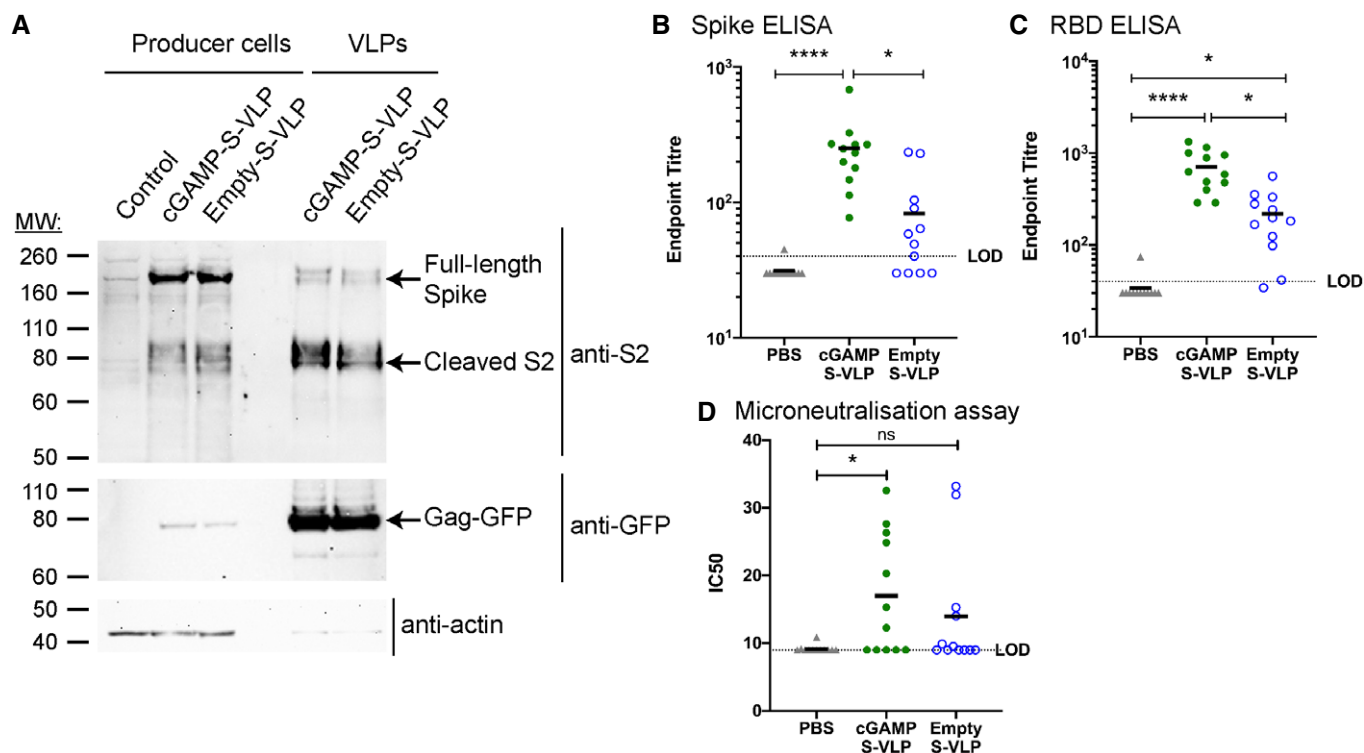


Figure 7. cGAMP-VLPs containing the SARS-CoV-2 S protein induce an enhanced antibody response.

- A** cGAMP-S-VLPs and Empty-S-VLPs incorporate SARS-CoV-2 S. Lysates from VLP producer cells and VLP preparations were analysed by Western blot for the presence of the S2 subunit of SARS-CoV-2 S, Gag-GFP and actin using the indicated antibodies.
- B, C** Immunisation with cGAMP-S-VLPs augments anti-Spike and anti-RBD antibody titres. Mice were immunised *via* the intra-muscular route with 5×10^5 IU of cGAMP-S-VLPs, Empty-S-VLPs or PBS as a control. Three weeks after immunisation, sera were collected, heat-inactivated, and titres of antibodies capable of binding to SARS-CoV-2 S (B) or its RBD (C) were determined by ELISA. The antibody response was expressed as end-point titre defined as the reciprocal of the highest serum dilution that gives a positive signal (blank+10SD). The dotted line shows the limit of detection (LOD).
- D** Immunisation with cGAMP-S-VLPs induces neutralising antibodies. Using serum samples from (B), antibody titres capable of neutralising SARS-CoV-2 were determined by microneutralisation (MN) assay. Calculated IC50 doses from multiple serum dilutions are shown. The dotted line shows the LOD.

Data information: Panel (A) is representative of two independent experiments. In (B–D), data were pooled from two independent experiments including a total of 12 mice per condition; symbols show data from individual animals. Horizontal lines indicate the mean. Statistical analyses were done using a Kruskal–Wallis test followed by Dunn’s multiple comparisons test (B, C, D). * $P < 0.05$; **** $P < 0.0001$. See also Fig EV5.

observation include that incorporating cGAMP inside viral particles (i) increases its stability at the site of injection by preventing degradation in the extracellular milieu (Li *et al*, 2014; Carozza *et al*, 2020) and/or (ii) prevents dilution by diffusion. Using small doses of cGAMP is likely to improve vaccine safety by limiting systemic inflammation. Indeed, we observed a transient weight loss of approximately 5% in mice receiving 10^6 infectious units of cGAMP-VLPs (containing ~ 50 ng of cGAMP) or the adjuvants AddaVax and poly(I:C), but not in Empty-VLP-immunised mice or in animals receiving lower—but nonetheless efficacious—doses of cGAMP-VLPs. Future development of cGAMP-VLPs, building on our proof-of-concept study, will be required to assess and further improve safety and stability of cGAMP-loaded viral-vectored vaccines for testing in human. The HIV-derived VLPs we used are related to lentiviral vectors. This will allow application of established techniques and protocols for industrial production and purification and will likely accelerate this development phase (Merten *et al*, 2016).

In an effort to protect CDNs, some reports described systems where CDNs are incorporated into micro- or nanoparticles (Hanson

et al, 2015; Chen *et al*, 2018; Junkins *et al*, 2018; Wang *et al*, 2020). Although these studies showed a higher *in vivo* efficacy of CDNs upon incorporation into particles, they nonetheless employed high amounts of CDNs, typically above 1 μ g. Furthermore, multiple immunisations were required, and only one study described a particle containing both antigen and CDN (Chen *et al*, 2018). In contrast, we demonstrate protective effects upon a single immunisation with VLPs containing both antigen and very low levels of cGAMP.

In addition to HIV-derived lentiviruses, other enveloped viruses also incorporate cGAMP (Bridgeman *et al*, 2015; Gentili *et al*, 2015). Therefore, our strategy of protecting the adjuvant cGAMP together with antigen in viral particles may be applicable to other viral-vectored vaccines such as modified vaccinia virus Ankara (MVA). cGAMP loading of viral-vectored vaccines is likely to be advantageous not only in terms of safety but also by reducing cost of vaccine production, due to the requirement for lower doses. The latter is particularly important for lentivirus-based vectors that can typically only be produced at lower titres than other viral-vectored vaccines.

HIV-derived VLPs are a flexible system that allows incorporation of proteins of choice. We demonstrate this by decorating VLPs with IAV HA and SARS-CoV-2 S and show that upon immunisation, these VLPs induced antibodies that neutralised IAV expressing a matched HA protein and SARS-CoV-2, respectively. In future, other pathogen-derived proteins could be incorporated into cGAMP-loaded VLPs as a strategy to produce vaccines for a diverse breadth of pathogens. For example, multiple HA proteins from different IAV clades could be incorporated to induce broadly protective responses and envelope proteins from other recently emerging viruses such as Zika or Ebola could be delivered using this approach. Furthermore, we envisage that envelope glycoproteins from future emerging viruses with pandemic potential could be used in our system, allowing for rapid testing of cGAMP-VLPs containing these proteins as candidate vaccines.

It is noteworthy that Empty-VLPs were not inert but induced adaptive immune responses, albeit at lower levels than cGAMP-VLPs. This effect may be due to the presence in VLP preparations of nucleic acid fragments from producer cells, which could mediate a degree of adjuvanticity via receptors such as TLR9 (Pichlmair *et al*, 2007). Both splenic CD4 effector T-cell responses and Tfh cell numbers in draining lymphoid tissues were enhanced by incorporation of cGAMP in VLPs. It is likely that these effects explain the increased antibody responses we observed against VLP proteins. The CD4 T-cell response was skewed towards a Th1 phenotype, as indicated by robust IFN γ and TNF α production by CD4 T cells and enhanced IgG2a/c and IgG2b antibody responses. This is in line with previous studies showing that 2'3'-cGAMP induces a predominantly Th1-biased response with weak Th2 induction (Blaauboer *et al*, 2015; Borriello *et al*, 2017; Wang *et al*, 2020). Both Empty-VLPs and cGAMP-VLPs also induced IgG1 responses raising the possibility that cGAMP-VLPs trigger Th1 responses via cGAMP and Th2 responses via other VLP components. This may broaden the application of this platform and should be investigated in future studies.

Both the cell type mediating antigen presentation and the cytokines produced at the time of T-cell activation are crucial for polarisation of T-cell responses (O'Garra, 1998; Itano & Jenkins, 2003; Hong *et al*, 2018). Notably, IFN-I and IL-6 production by DCs have been reported to induce the development of Tfh cells in mice (Cucak *et al*, 2009; Nurieva *et al*, 2009; Riteau *et al*, 2016). We previously found that cGAMP-loaded viruses induce IFN-I in bone marrow-derived macrophages *in vitro* (Bridgeman *et al*, 2015). The activation of STING and down-stream IRF3 and NF- κ B signalling by

cGAMP *in vivo* might therefore trigger production of IFN-I and IL-6 that could underlie the potent CD4 Tfh response elicited following immunisation with cGAMP-VLPs. The VLPs used here were pseudotyped with VSV-G, which has a broad tropism (Finkelshtein *et al*, 2013; Hastie *et al*, 2013). Many cell types may therefore be infected at the site of injection (the muscle) and respond to cGAMP. Other types of VLPs such as Q β -VLPs travel through the lymphatics to draining lymph nodes (Mohsen *et al*, 2017). Although larger than Q β -VLPs, HIV-derived VLPs might also reach lymph nodes where they could infect other cell types. The specific cell types infected by VLPs *in vivo* and the cytokines induced by these cells are likely to be key aspects of the response induced by cGAMP-VLPs *in vivo* and warrant further investigation. It is also possible to replace VSV-G with other envelope proteins that target VLPs to specific cell types. For example, the envelope protein from Sindbis virus or antibodies such as those to DEC205 target virus particles to DCs, an essential antigen-presenting cell type (Trumpfheller *et al*, 2006; Yang *et al*, 2008). It will be interesting to determine whether DC-targeted VLPs containing cGAMP have a similar effect on the responses induced compared with the VSV-G pseudotyped VLPs described here. DC targeting could improve vaccine efficacy by restricting cGAMP delivery to relevant antigen-presenting cells.

Many studies are currently aimed at designing vaccines that induce antigen-specific CD8 T cells (Panagiotti *et al*, 2018). We found that cGAMP loading of VLPs enhanced CD8 T-cell responses to the internal HIV-Gag antigen. However, the increased response in cGAMP-VLP-immunised mice did not result in a significant improvement in protection against a vaccinia virus expressing the same HIV-Gag compared with that observed in animals vaccinated with Empty-VLPs. The immunisation route and schedule employed here consisted of a single dose of VLPs injected intra-muscularly, which might not be adequate to elicit sufficiently high-magnitude CD8 T-cell responses to confer protection, but deployment in prime-boost regimens should be explored. In light of the neutralising antibody response induced by cGAMP-loaded VLPs, heterologous booster immunisations using non-particulate vaccines or viral particles with a different envelope protein should be considered in the future.

In summary, we provide proof-of-concept evidence that vaccination with HIV-derived VLPs containing both the adjuvant cGAMP and protein antigens constitutes an efficacious platform for induction of CD8 T-cell and neutralising antibody responses at low VLP doses. This VLP-based strategy of coupling adjuvant and antigen in a single entity is therefore a promising approach for future development of new and safer vaccines against a range of pathogens.

Materials and Methods

Reagents and Tools table

Reagent/Resource	Reference or source	Identifier or catalog number
Experimental models		
HEK293T (<i>H. sapiens</i>)	Caetano Reis e Sousa lab	N/A
HEK293 (<i>H. sapiens</i>)	Caetano Reis e Sousa lab	N/A
3C11 (<i>H. sapiens</i>)	Bridgeman et al (2015)	N/A
143B (<i>H. sapiens</i>)	Nick Proudfoot lab	N/A

Reagents and Tools table (continued)

Reagent/Resource	Reference or source	Identifier or catalog number
THP-1 (<i>H. sapiens</i>)	Vincenzo Cerundolo lab	N/A
MDCK-SIAT1 (<i>C. familiaris</i>)	ECACC Matrosovich et al (2003)	05071502
MDCK-PR8 (<i>C. familiaris</i>)	Powell et al (2012)	N/A
VERO (<i>C. aethiops</i>)	ATCC	CCL-81
C57BL/6j (<i>M. musculus</i>)	Envigo	057
C57BL/6 (<i>M. musculus</i>)	University of Oxford Biomedical Services	N/A
C57BL/6 <i>Tmem173</i> ^{-/-} (<i>M. musculus</i>)	Jin et al (2011)	N/A
Influenza virus H1N1 A/Puerto Rico/8/1934 (Cambridge) (PR8)	Townsend lab. Virus produced in house via reverse genetics. Reference for the sequences: Winter et al (1981)	N/A
S-FLU vector expressing eGFP (S-eGFP)	Powell et al (2012)	N/A
Vaccinia virus vV1	Borrow et al (1994)	N/A
SARS-CoV-2 Victoria/01/2020	Caly et al (2020)	N/A
Recombinant DNA		
pGag-EGFP	NIH AIDS Reagent program	Cat #11468
pCMV-VSV-G	Addgene	Cat #8454
pcDNA3-Flag-mcGAS	Sun et al (2013)	N/A
pcDNA3-Flag-mcGAS-G198A/S199A	Sun et al (2013)	N/A
pcDNA3.1-H1 (PR8)	Original sequence from Winter et al (1981)	N/A
pcDNA3.1-Spike	Made in Townsend lab: codon-optimised Spike cDNA (genbank QHD43416.1) was synthesized by GeneArt and cloned into pcDNA3.1	N/A
pNL4-3-deltaE-EGFP	NIH AIDS Reagent program	Cat #11100
Antibodies		
CD16/CD32 Rat anti-mouse Clone: 93	eBioscience	Cat #14-0161-82
PE-Cy7 IFN γ rat anti-mouse Clone: XMG1.2	eBioscience	Cat # 25-7311-82
BrilliantViolet 605 anti-mouse CD8a Clone: 53-6.7	Biolegend	Cat # 100743
PerCP-Cy5.5 anti-mouse CD90.2 Clone: 30-H12	Biolegend	Cat # 105337
AlexaFluor 700 anti-mouse CD4 Clone: RM4-5	Biolegend	Cat # 100536
BrilliantViolet 510 anti-mouse MHC-II (I-A/I-E) Clone: M5/114.15.2	Biolegend	Cat # 107635
PE anti-mouse TNF α Clone: MP6-XT22	Biolegend	Cat # 506305
APC anti-mouse IL2 Clone: JES6-5H4	Biolegend	Cat # 503809
APC-Cy7 anti-mouse B220 Clone: RA3-6B2	Biolegend	Cat # 103223
BrilliantViolet 510 anti-mouse B220 Clone: RA3-6B2	Biolegend	Cat # 103247
PerCP-Cy5.5 anti-mouse IgD Clone: 11-26c.2a	Biolegend	Cat # 405709
AlexaFluor 647 GL7	Biolegend	Cat # 144605
PerCP-Cy5.5 anti-mouse CD44 Clone: IM7	Biolegend	Cat # 103031
BrilliantViolet 421 anti-mouse CXCR5 Clone: L138D7	Biolegend	Cat # 145511
APC anti-mouse PD1	Biolegend	Cat # 109111

Reagents and Tools table (continued)

Reagent/Resource	Reference or source	Identifier or catalog number
Clone: RMP1-30		
PE anti-mouse CD95 Clone: Jo2	BD Bioscience	Cat # 561985
AlexaFluor 647 goat-anti mouse antibody	Life Technology	Cat # A21235
HRP goat anti-mouse IgG1	Bethyl laboratories	Cat # A90-205P
HRP goat anti-mouse IgG2a/c	Bethyl laboratories	Cat # A90-207P
HRP goat anti-mouse IgG2b	Bethyl laboratories	Cat # A90-109P
HRP goat anti-mouse IgM	Bethyl laboratories	Cat # A90-201P
HRP goat anti-mouse	Agilent	Cat # P0447
Anti-IAV Hemagglutinin H1 & H5 Clone: 21-D8-5A	Xiao et al (2018)	N/A
Anti-SARS-CoV-2 Spike (S2 subunit) Clone: FD-10A	Townsend lab, Huang et al (2021)	N/A
Mouse anti-GFP	Roche	Cat # 11814460001
HRP anti-actin	Sigma	Cat # A3854
Chemicals, Enzymes and other reagents		
LIVE/DEAD fixable violet dead cell stain	ThermoFischer scientific	Cat # L34955
LIVE/DEAD fixable aqua dead cell stain	ThermoFischer scientific	Cat # L34957
HIV-1 Con B Gag Peptide Set	NIH AIDS Reagent Program	Cat # 8117
pep 92 9-mer (HIV-SQV)	Genscript	Custom synthesis
pep 92 10-mer	Genscript	Custom synthesis
pep 92 11-mer	Genscript	Custom synthesis
Recombinant HIV-1 IIIB pr55 Gag protein	NIH AIDS Reagent Program	Cat # 3276
Recombinant VSV-G protein	alpha diagnostic international	Cat # VSIG15-R-10
2'3'-cGAMP	Invivogen	Cat # tlrl-nacga23
2'3'-cGAMP VacchiGrade	Invivogen	Cat # vac-nacga23
Poly(I:C) (HMW)	Invivogen	Cat # tlrl-pic
AddaVax	Invivogen	Cat # vac-adx-10
Brilliant stain buffer	BD Bioscience	Cat # 563794
Fixation/Permeabilisation Solution kit with GolgiStop	BD Bioscience	Cat # 554715
eBioscience FoxP3/transcription factor staining Buffer Set	ThermoFischer scientific	Cat # 00-5523-00
BD Cellfix	BD Bioscience	Cat # 340181
Fugene 6	Promega	Cat # E2691
Lipofectamine 2000	ThermoFischer scientific	Cat # 11668030
One-Glo luciferase assay system	Promega	Cat # E6120
Amicon Ultra 3K filter columns	Millipore	Cat # UFC500396
2'-3' cGAMP ELISA kit	Cayman chemical	Cat # 501700
Mouse IFN γ ELISPOT BASIC (ALP) kit	Mabtech	Cat # 3321-2A
Mouse IgG Basic ELISPOT BASIC (ALP) kit	Mabtech	Cat # 3825-2A
Red blood cell lysis buffer	Sigma	Cat # R7757-100ML
TMB substrate	Invitrogen	Cat # 00-4201-56
BM Blue POD substrate	Roche	Cat # 11484281101
TPCK-treated trypsin	Sigma	Cat # T1426
Software		
FlowJo v10.7.1		
Graphpad Prism v8.4.3		

Methods and Protocols

Mice

All mice were on the C57BL/6 background. Only female mice between 6 and 8 weeks old were used. Animals were housed in individually ventilated cages and standard husbandry conditions were used. WT mice were obtained from University of Oxford Biomedical Services or Envigo RMS (UK) Limited. *Tmem173*^{-/-} (STING-deficient; herein referred to as *Sting*^{-/-} for simplicity) mice were a gift from J Cambier (Jin *et al*, 2011). This work was performed in accordance with the UK Animals (Scientific Procedures) Act 1986 and institutional guidelines for animal care. This work was approved by project licences granted by the UK Home Office (PPL No. 40/3583, No. PC041D0AB and No. PBA43A2E4) and was also approved by the Institutional Animal Ethics Committee Review Board at the University of Oxford.

Cells

Cell lines (HEK293T, HEK293, 3C11, 143B, MDCK-SIAT1, MDCK-PR8, VERO) were maintained in DMEM (Sigma-Aldrich) supplemented with 10% FCS (Sigma-Aldrich) and 2 mM L-glutamine (Gibco) at 37°C and 5% CO₂. 3C11 cells are HEK293 cells stably transduced with an ISRE-Luc reporter construct (Bridgeman *et al*, 2015). 143B cells were a kind gift from N. Proudfoot (University of Oxford).

Bone marrow cells were isolated from humanely killed adult mice by standard protocols and grown in 6-well plates for 5 days in RPMI supplemented with 10% FCS, 2 mM L-glutamine, 1% PenStrep and 20 ng/ml mouse GM-CSF to obtain bone marrow-derived myeloid cells (BMMCs).

Reagents and antibodies

See Reagents and Tools Table.

VLP and HIV-1 vector production

All VLPs were produced by transient transfection of HEK293T cells with Eugene 6. HEK293T were seeded into 15-cm dishes to reach 60–70% confluency the next day, and VLPs were produced by co-transfecting plasmids encoding Gag-eGFP and the VSV-G envelope (pGag-EGFP and pCMV-VSV-G, respectively) at a ratio of 2:1. VLPs were loaded with cGAMP by co-transfecting at the same time a plasmid encoding mouse cGAS WT (pcDNA3-Flag-mcGAS). Empty-VLPs were produced as control by co-transfecting a catalytically inactive mouse cGAS (cGAS AA; pcDNA3-Flag-mcGAS-G198A/S199A). One day after transfection, the medium was changed. Supernatants were collected 24, 32 and 48 h after medium change, centrifuged and filtered (cellulose acetate membrane 0.45 µm pore-size). At each media change, VLPs were concentrated by ultracentrifugation through a 20% sucrose cushion at 90,000 g for 2.5 h at 8°C using a Beckman SW32 rotor. VLPs were resuspended in PBS, and subsequent harvests were resuspended using the resuspended VLPs from previous harvests to maximise titre.

For pseudotyping cGAMP-VLPs and Empty-VLPs with influenza haemagglutinin H1 (HA; pcDNA3.1-H1 (PR8)), cells were transfected as above with the following plasmids: Gag-eGFP, VSV-G, HA and cGAS WT or AA at a ratio of 2:1:1:2. For pseudotyping cGAMP-VLPs and Empty-VLPs with SARS-CoV-2 Spike (S; pcDNA3.1-Spike), cells were transfected with the following plasmids: Gag-eGFP, VSV-G, S and cGAS WT or AA at a ratio of 2:1:1:2.

To produce VSV-G pseudotyped HIV-1 vectors for neutralisation assays, HEK293T cells were co-transfected with the following plasmids: HIV-1 NL4-3 ΔEnv GFP (pNL4-3-deltaE-EGFP) and VSV-G at a ratio of 2:1.

VLP titration and cGAMP incorporation assays

HEK293 cells were seeded at a density of 1×10^5 cells per well in 24-well plates. The next day, cells were infected with decreasing amounts of VLPs in the presence of 8 µg/ml of polybrene. 24 h after infection, cells were collected and first stained with anti-CD16/32 and Aqua fixable Live/Dead in FACS Buffer (PBS, 1% FCS, 2mM EDTA) for 15 min at RT. Cells used for titration of HA-VLPs were also stained for HA using a primary human anti-H1 & H5 antibody (clone 21-D8-5A) in FACS Buffer for 30 min at 4°C. Cells were then washed twice and further stained with a secondary goat anti-human Alexa Fluor 647-conjugated antibody for 30 min at 4°C, followed by two washes. All cells were fixed using BD Cellfix before acquisition on an Attune Nxt flow cytometer. Infection was measured by analysing GFP-positive cells by flow cytometry using FlowJo version 10. VLP titres were calculated based on the number of GFP⁺ cells compared with the number of cells in the well at the time of infection and expressed as infectious units/ml (IU/ml). Supernatants from infected cells were transferred onto ISRE reporter cells to assess IFN-I production in response to cGAMP incorporated in VLPs as described previously (Bridgeman *et al*, 2015). After 24 h of incubation with supernatants, expression of the ISRE-Luc reporter was assessed using the One-Glo luciferase assay system.

Small molecular extracts were prepared from VLPs as described (Mayer *et al*, 2017). Briefly, 2×10^6 IU of ultra-centrifuged VLPs resuspended in PBS were lysed in X-100 Buffer (1 mM NaCl, 3 mM MgCl₂, 1mM EDTA, 1% Triton X-100, 10 mM Tris pH7.4) by adding 1/10 volume of 10× buffer for 20 min on ice while vortexing regularly. After centrifugation at 1,000 g for 10 min at 4°C, supernatants were treated with 50 U/ml of benzonase for 45 min on ice. Samples were then extracted with phenol–chloroform, and the aqueous phase was then transferred to Amicon Ultra 3K filter columns. After filtering by centrifugation at 14,000 g for 30 min at 4°C, samples were dried in a SpeedVac and resuspended in 200 µl of water. cGAMP was quantified using the 2′–3′ cGAMP ELISA kit following the manufacturer's instructions and the cGAMP bioassay as described previously (Bridgeman *et al*, 2015). Briefly, THP-1 cells were seeded in the presence of 5 ng/ml PMA. The next day, small molecular extracts were delivered to the cells using a permeabilisation buffer (2× PERM: 100 mM HEPES-HCl (pH 7.4), 200 mM KCl, 6 mM MgCl₂, 0.4% BSA, 170 mM sucrose, 2 mM ATP, 0.2 mM GTP, 0.002% digitonin) alongside a cGAMP standard. After 30 min of incubation at 37°C, cells were washed, fresh medium was added and the cells were placed back in the incubator for an additional 24 h. IFN-I produced was quantified using an ISRE reporter assay and the quantity of cGAMP was calculated using the cGAMP standard. For both assays, a small molecular extract of a control sample containing 1 µg of chemically synthesised cGAMP was used to normalise the quantities of cGAMP in the VLP samples.

IAV

The influenza virus H1N1 A/Puerto Rico/8/1934 (Cambridge) (PR8) and the non-replicating S-FLU vector expressing eGFP (S-eGFP) were generated as previously described (Powell *et al*, 2012).

Plasmids encoding the IAV Cambridge strain of A/Puerto Rico/8/34 were used to generate the wild-type H1N1 A/Puerto Rico/8/1934 (Cambridge) (PR8) seed virus. The same plasmids were used to generate the PR8 S-eGFP with slight modifications: the HA coding region in the plasmid expressing HA viral RNA was replaced with eGFP and an additional plasmid was included to provide a functional PR8 HA in *trans* to rescue the PR8 S-eGFP seed virus. Briefly, the plasmids were transfected into HEK293T cells using Lipofectamine 2000 and supernatant containing seed virus was collected 72 h after transfection. The wild-type PR8 virus and the S-eGFP vector were then propagated by infecting MDCK-SIAT1 cells or MDCK-SIAT1 stably transfected with PR8 HA (MDCK-PR8), respectively, with seed virus, followed by medium change into VGM (Viral Growth Media; DMEM, 1% BSA, 10 mM HEPES buffer, 1% PenStrep) containing 1 µg/ml TPCK-treated trypsin. Viruses were harvested 48 h later. The TCID₅₀ was determined by infecting MDCK-SIAT1 or MDCK-PR8 cells with a ½-log dilution series of viruses in VGM for 1 h in eight replicates using 96-well flat-bottom plates. Next, 150 µl per well of VGM with TPCK-treated trypsin (1 µg/ml) was added and cells were further incubated for 48 h at 37°C. The PR8 virus and the S-eGFP vector were quantified by nucleoprotein (NP) staining and eGFP expression, respectively, and TCID₅₀ was calculated using the method of Reed and Muench (Reed & Muench, 1938).

Vaccinia virus

Stocks of the vaccinia virus expressing HIV-1 HXB.2 Gag (vVK1) were produced by growth in 143TK cells, and infectious virus titres were determined by plaque assay (Borrow *et al*, 1994).

Immunisation and viral challenge of mice

Animals were injected intra-muscularly with 50 µl per hindleg of PBS or 10⁶ IU of cGAMP-VLPs or Empty-VLPs, unless otherwise stated, under inhalation isoflurane (IsoFlo, Abbott) anaesthesia. For comparisons with other adjuvants, when indicated, mice were immunised with 10⁶ IU of Empty-VLPs mixed with 25 µg poly(I:C) (HMW), or with 5 × 10⁴ IU of Empty-VLPs with AddaVax (1:1 v/v). Weight was monitored every day for 14 days. For immunophenotyping, mice were culled on day 14 by inhalation of carbon dioxide and cervical dislocation. For viral challenge experiments, mice were monitored every other day for an additional 2 weeks before challenge.

For IAV challenge, blood samples were acquired 2 weeks after immunisation for evaluation of the serum antibody response. Mice were then challenged a month after immunisation *via* the intranasal route with 10,000 TCID₅₀ of PR8 diluted in 50 µl VGM under inhalation isoflurane anaesthesia. Weight was monitored daily, and mice were culled by inhalation of carbon dioxide and cervical dislocation when body weight loss approached the humane end-point of 20%.

For vaccinia virus challenge, mice were infected *via* the intraperitoneal route with 10⁶ PFU vVK1 in 100 µl PBS. Weight was monitored daily for 5 days. Animals were then culled by inhalation of carbon dioxide and cervical dislocation, and ovaries were collected for virus titration.

Analysis of T-cell responses by ICS and ELISPOT

Splenocytes were obtained by separating spleens through a 70-µm strainer and were then treated with red blood cell lysis buffer for

5 min, washed and resuspended in RPMI supplemented with 2% human serum, 2 mM L-glutamine, 1% PenStrep (R2).

For ELISPOT assays, splenocytes were seeded in R2 at a density of 1.5 × 10⁵ cells per well on ELISPOT plates pre-coated with anti-IFNγ detection antibody. Cells were either non-treated or treated with 2 µg/ml HIV-1 Gag peptide or with 10 ng/ml PMA and 1 µg/ml ionomycin as a control, and incubated for 48 h at 37°C before detection according to the manufacturer's instructions (Mouse IFNγ ELISPOT BASIC (ALP) kit).

For intracellular cytokine staining (ICS), cells were seeded in R2 at a density of 1 × 10⁶ cells per well in a round-bottom 96-well plates. Cells were either non-treated or treated with 2 µg/ml HIV-SQV 9-mer peptide or co-cultured with BMMCs pulsed overnight with cGAMP-VLP at a multiplicity of infection of 1. Cells were also treated with 10 ng/ml PMA and 1 µg/ml ionomycin as a positive control. After 1 h of incubation at 37°C, Golgi STOP was added according to manufacturer's instructions. After a further 5 h of incubation at 37°C, cells were washed twice in FACS buffer (PBS, 1% FCS, 2mM EDTA), incubated with anti-CD16/32 and Aqua or violet fixable Live/Dead in FACS Buffer for 15 min at RT and were then washed twice in FACS Buffer. Subsequent extracellular staining involved incubation of cells for 30 min at 4°C with the following antibodies: anti-CD8 BV605 and anti-CD90.2 PerCP-Cy5.5 in FACS Buffer for CD8 T-cell analysis in cells stimulated with the HIV peptide, or anti-CD4 AF700, anti-CD8 BV605 and anti-MHC-II BV510 in Brilliant stain buffer for CD4 T-cell analysis in cells stimulated with pulsed BMMCs. Cells were then washed twice in FACS Buffer and fixed using BD Cytotfix/Cytoperm buffer for 20 min at 4°C. After two washes in FACS Buffer with 10% BD Cytoperm/wash, intracellular staining was performed for using anti-TNFα PE, anti-IFNγ PE-Cy7 and anti-IL2 APC in FACS Buffer with 10% BD Cytoperm/wash for 30 min at 4°C. After two washes in FACS Buffer with 10% BD Cytoperm/wash, cells were fixed for 10 min at RT in BD Cellfix, washed again and resuspended in FACS Buffer for acquisition on Attune NxT flow cytometers. Analysis was performed using FlowJo version 10. Gates for phenotypic markers of CD4 and CD8 T cells were based on FMO controls. Unstimulated control cells were used for other gates.

Analysis of serum antibody titres by ELISA

Anti-VLP, anti-VSV-G and anti-Gag ELISAs

To extract protein, VLPs were lysed in PBS containing 0.5% Triton X-100 and 0.02% sodium azide for 10 min at RT. Quantity of protein extracted was quantified by BCA assay.

Costar high-binding half-area flat-bottom 96-well plates were coated overnight at 4°C with either 10 µg/ml unconcentrated cGAMP-VLP lysates, 1 µg/ml concentrated cGAMP-VLP lysates, 0.5 µg/ml recombinant HIV-1 IIIB pr55 Gag protein or 1.5 µg/ml recombinant VSV-G protein. The next day, plates were washed twice in PBS, then twice in PBS with 0.1% Tween-20 (wash buffer) and blocked in PBS with 3% BSA for 2 h at RT. Sera collected on day 14 after immunisation were serially diluted in PBS with 0.5% BSA starting at a dilution of 1/200 and diluting 1/3. After four washes in wash buffer, serum dilutions were added to the plates in duplicates (25 µl per well) and incubated for 1 h at 37°C. Plates were washed four times in wash buffer. Next, 50 µl per well of HRP-conjugated antibodies recognising different antibody classes or

subclasses was added using the following dilutions: goat anti-mouse IgG1 / IgG2a/c / IgG2b, 1/10,000; IgM, 1/2,000 in PBS with 0.5% BSA and incubated for 1 h at RT. Plates were washed four times in wash buffer, and 50 μ l of TMB substrate was added per well. Plates were incubated for approximately 30 min or until the signal was saturating, and 50 μ l of STOP solution was added per well before reading absorbance at 450 and 570 nm on a CLARIOstar plate reader.

SARS-CoV-2 S ELISA

To detect antibodies binding to SARS-CoV-2 S, we created MDCK-S cells by stably transducing parental MDCK-SIAT1 cells with a lentiviral vector expressing full-length SARS-CoV-2 S (Huang et al, 2021). MDCK-S cells were seeded into flat-bottom 96-well plates (3×10^4 cells per well) and incubated at 37°C overnight. Cells were then washed twice with PBS. Heat-inactivated mouse sera were serially diluted in PBS/0.1% BSA, and 50 μ l was added to the cells for 1 h at RT. Plates were then washed twice with PBS, and 50 μ l AlexaFluor 647-conjugated goat anti-mouse antibody (1:500 in PBS/0.1% BSA) was added per well for 1 h at RT. Plates were then washed twice with PBS, and 100 μ l of PBS/1% formalin was added per well. Fluorescence signals were acquired on a CLARIOstar plate reader. The S-specific antibody response was calculated as end-point titre (EPT). EPT is defined as the reciprocal of the highest serum dilution that gives a positive signal (blank+10SD) determined using a five-parameter logistic equation.

SARS-CoV-2 RBD ELISA

NUNC plates were coated with 50 μ l purified RBD-His₆ (2 μ g/ml in PBS) at 4°C overnight. Plates were then washed with PBS and blocked with 300 μ l of 5% skimmed milk for 1 h at RT. Blocked plates were then washed with PBS. Heat-inactivated mouse sera were serially diluted in PBS/0.1% BSA, and 50 μ l was transferred to the plates for 1 h at RT. Plates were then washed with PBS, and 50 μ l of secondary HRP-conjugated goat anti-mouse antibody (1:800 in PBS/0.1% BSA) was added per well for 1 h at RT. Plates were washed with PBS, and 50 μ l of BM Blue POD substrate was added for 5 min. The reaction was stopped by adding 50 μ l of 1 M H₂SO₄. OD450 was read on a CLARIOstar plate reader. EPT was determined as above. This ELISA to detect RBD-specific antibodies is described in detail in Huang et al (2021).

Analysis of germinal centre B cells and T follicular cells in draining lymph nodes

Both inguinal lymph nodes were meshed through a 70- μ m strainer. 10^6 cells per animal were used for each staining.

For germinal centre B-cell analysis, cells were first stained with anti-CD16/32 and Aqua fixable Live/Dead in FACS Buffer for 15 min at RT. After two washes in FACS Buffer, extracellular staining was performed using anti-B220 APC-Cy7, anti-CD95 PE, anti-IgD PerCP-Cy5.5 and GL7 AF647 in FACS Buffer for 30 min at 4°C. Cells were then washed, fixed for 10 min at RT in BD Cellfix, washed again and resuspended in FACS Buffer.

For T follicular cell analysis, cells were first stained with anti-CD16/32 and Aqua fixable Live/Dead in FACS Buffer for 15 min at RT. After two washes in FACS Buffer, extracellular staining was performed using anti-B220 BV510, anti-CD4 AF700, anti-CD44

PerCP-Cy5.5, anti-CXCR5 BV421 and anti-PD-1 APC in Brilliant stain buffer for 1 h at 4°C. After two washes in FACS Buffer, cells were fixed using the eBioscience FoxP3 fixation buffer for 25 min at RT. Cells were then washed twice in cold eBioscience Perm buffer, and intracellular staining was performed using anti-FoxP3 PE-Cy7 in eBioscience Perm buffer for 40 min at RT. After two washes in eBioscience Perm buffer, cells were then fixed for 10 min at RT in BD Cellfix, washed again and resuspended in FACS Buffer for acquisition on Attune NxT flow cytometers. Analysis was performed using FlowJo version 10. Gates for phenotypic markers of CD4 T cells and B cells were based on FMO controls, and gates for GC and Tfh/Tfr markers were based on PBS-immunised mice.

B cell ELISPOT

Cells from spleen and draining lymph nodes were collected as described above and counted. Three different amounts of cells (10^6 , 3×10^5 , 1×10^5) were seeded in duplicate in R2 on ELISPOT plates coated overnight with 2 μ g/ml of lysates from cGAMP-VLPs (see ELISA). Plates were then incubated overnight at 37°C before detection according to manufacturer's instruction (Mouse IgG Basic ELISPOT BASIC (ALP) kit). Analysis was performed using the cell density showing the least background in PBS-injected mice.

IAV microneutralisation assay

Microneutralisation (MN) assay was performed as described (Powell et al, 2012) with minor modifications. Briefly, a single cycle IAV expressing eGFP (S-eGFP (PR8)) containing the H1 haemagglutinin was titrated to give saturating infection of 3×10^4 MDCK-SIAT1 cells per well in 96-well flat-bottom plates, detected by eGFP fluorescence. Murine sera were heat inactivated for 30 min at 56°C. Dilutions of sera were incubated with S-eGFP for 2 h at 37°C before addition to 3×10^4 MDCK-SIAT1 cells per well. Cells were then incubated overnight before fixing in 4% formaldehyde. The suppression of infection was measured on fixed cells by fluorescence on a CLARIOstar fluorescence plate reader.

SARS-CoV-2 MN assay

Heat-inactivated mouse sera were serially diluted in DMEM+1% FBS and then incubated with live SARS-CoV-2 for 90 min at RT, using a concentration of virus that yields approximately 100 foci per well. 4.5×10^4 Vero ATCC (CCL81) cells were then added to each well. After 2 h of incubation, the cells were overlaid with DMEM+1% FBS containing CMC at a final concentration of 1.5%. Cells were then incubated for 20 h before fixation with 4% PFA for 30 min at RT. Cells were then permeabilised with PBS+2% Triton X-100 for 30 min at 37°C before staining with an antibody targeting the SARS-CoV-2 Nucleocapsid (clone EY-2A) for 1 h at RT, followed by an HRP-coupled anti-human IgG antibody. Infected cells were revealed using TrueBlue peroxidase substrate incubated for 10 min at RT. Plates were then washed with water and counted with an ELISPOT plate reader. The number of spots per well was normalised to wells that received no serum and the IC50 was calculated in Prism using a non-linear regression [inhibitor] vs normalised response—variable slope. This work was performed in a BSL3 laboratory and details of the MN assay will be described in Harding, A. & Gilbert-Jaramillo, J. et al (manuscript in preparation).

Western blot

Cells were lysed in NP-40 buffer (150 mM NaCl, 1% NP-40, 50 mM Tris pH 8.0) with protease inhibitors. After 20 min of incubation on ice, lysates were centrifuged at 17,000 g for 10 min at 4°C. Supernatant was collected and diluted with sample buffer containing beta-mercaptoethanol before denaturation at 95°C for 5 min. Samples were loaded on pre-cast 4–12% gradient Bis-Tris protein gels that were run with MOPS buffer at 120 volts for 2 h. Transfer to nitrocellulose membranes was performed in transfer buffer (25 mM Tris, 192 mM glycine, 10% methanol) at 90 volts for 2 h. Membranes were blocked in 5% milk powder in Tris-buffered saline with 0.05% NP-40 (TBSN) for 1 h at room temperature, then washed five times for 5 min in TBSN. Membranes were incubated with primary antibody in 5% milk TBSN overnight at 4°C and washed five times for 5 min in TBSN. Membranes were then incubated with HRP-coupled secondary antibody in 5% milk TBSN for 1 h at room temperature and washed five times for 5 min in TBSN. Western Lightning Plus-ECL substrate was used for signal detection on an iBright FL1000 machine. In some experiments, membranes were stripped with 0.2 M glycine, 1% SDS at pH 2.5 for 15 min, washed, blocked and re-probed with a different antibody.

Vaccinia virus plaque assay

Ovaries collected in D0 (DMEM, 1% PenStrep) were homogenised using glass beads in screw cap tubes in a homogeniser (two cycles at speed 6.5 for 30 s). Samples were then placed on ice for 1–2 min, and homogenisation was repeated. Samples were then subjected to three freeze-thaw cycles between 37°C and dry ice and sonicated three times for 30 s with 30-s intervals on ice. Supernatants containing virus were collected in new tubes after centrifugation at 9,600 g for 3 min at 4°C.

143B cells were seeded in 12-well plates at a density of 0.25×10^6 cells per well in 1 ml D10. The next day, log serial dilutions of virus-containing samples were prepared in D0. Supernatant was replaced with 550 µl of diluted virus-containing samples and incubated for 2 h at 37°C, swirling plates every 30 min to avoid drying. Virus containing samples were then removed, and cells were covered in 1.5 ml of D10 containing 1% Pen/Strep and 0.5% carboxymethylcellulose (CMC). Forty-eight hours after infection, cells were carefully washed with PBS and fixed in 4% formaldehyde for 20 min at RT before staining with 0.5% crystal violet.

Statistics

Statistical analysis was performed in GraphPad Prism v7.00 as detailed in the figure legends.

Data availability

The authors declare that all data supporting the findings of this study are available within the paper and its associated files. No primary data sets have been generated or deposited.

Expanded View for this article is available online.

Acknowledgements

The authors thank William James for providing access to the BSL3 facility and for his support in developing the MN assay for SARS-CoV-2. We further thank

Andrew McMichael, Adrian Hill, Michelle Linterman, Daniel Radtke, Oliver Bannard, Nicolas Manel, Rachel E. Rigby and members of the Rehwinkel lab for discussion. The authors thank Uzi Gileadi and Vincenzo Cerundolo for their help with IAV infections. The authors thank Nicholas Proudfoot and Bernard Moss for providing, respectively, the 143B cells and the vVK1 vaccinia virus. The following reagents were obtained through the NIH AIDS Reagent Program, Division of AIDS, NIAID, NIH: HIV-1 Con B Gag Peptide Set, HIV-1 HXB2 Gag-EGFP Expression Vector (Cat#11468) from Dr. Marilyn Resh, HIV-1 NL4-3 ΔEnv EGFP Reporter Vector from Drs. Haili Zhang, Yan Zhou, and Robert Siliciano (cat# 11100), HIV-1IIIIB pr55 Gag. This work was funded by the UK Medical Research Council [MRC core funding of the MRC Human Immunology Unit, MC_UU_00008/1; J.R., J.F., H.D. and MRC Programme grant, MR/K012037; P.B.], the Wellcome Trust [grant number 100954; J.R.], and the NIH, NIAID, DAIDS [UM1 grants AI00645 (Duke CHAVI-ID) and AI144371 (Duke CHAVD); P.B.]. P.B. is a Jenner Institute Investigator. J.G.-J. is funded by the National Ecuatorian Governemnt—Secretaría Nacional de Educación Superior, Ciencia, Tecnología y Educación—SENESCYT. M.L.K. is funded by the Biotechnology and Biological Sciences Research Council (BBSRC) [grant number BB/M011224/1]. R.A.R. acknowledges the generous support of philanthropic donors that allowed funding from the University of Oxford's COVID-19 Research Response Fund, which also supported the SARS-CoV-2 BSL3 facility and microneutralisation assay. Initial funding for the Virus Screening Facility was provided by the Oxford BRC and Cancer Research UK. The funders had no role in study design, data collection and analysis, decision to publish or preparation of the manuscript.

Author contributions

LC, AB and JR conceptualised the study; LC, AB, TKT, PR, JF, IP-P, TP, JG-J, MLK, XL and RAR contributed to methodology; n.a. provided software; LC and JR validated the study; LC and JR involved in formal analysis; LC, AB, TKT and JF investigated the study; RB and PB provided resources; LC curated the data; LC and JR wrote—original draft; all authors wrote—review & editing; LC and JR visualised the study; JR, AT, HD and PB supervised the study; LC involved in project administration; JR contributed to funding acquisition.

Conflict of interest

The authors declare that they have no conflict of interest.

References

- Ablasser A, Goldeck M, Cavlar T, Deimling T, Witte G, Rohl I, Hopfner KP, Ludwig J, Hornung V (2013) cGAS produces a 2'-5'-linked cyclic dinucleotide second messenger that activates STING. *Nature* 498: 380–384
- Blaauboer SM, Gabrielle VD, Jin L (2014) MPYS/STING-mediated TNF-alpha, not type I IFN, is essential for the mucosal adjuvant activity of (3'-5')-cyclic-di-guanosine-monophosphate in vivo. *J Immunol* 192: 492–502
- Blaauboer SM, Mansouri S, Tucker HR, Wang HL, Gabrielle VD, Jin L (2015) The mucosal adjuvant cyclic di-GMP enhances antigen uptake and selectively activates pinocytosis-efficient cells in vivo. *Elife* 4: e06670
- Borriello F, Pietrasanta C, Lai JCY, Walsh LM, Sharma P, O'Driscoll DN, Ramirez J, Brightman S, Pugni L, Mosca F *et al* (2017) Identification and characterization of stimulator of interferon genes as a robust adjuvant target for early life immunization. *Front Immunol* 8: 1772
- Borrow P, Lewicki H, Hahn BH, Shaw GM, Oldstone MB (1994) Virus-specific CD8+ cytotoxic T-lymphocyte activity associated with control of viremia in primary human immunodeficiency virus type 1 infection. *J Virol* 68: 6103–6110

- Bridgeman A, Maelfait J, Davenne T, Partridge T, Peng Y, Mayer A, Dong T, Kaefer V, Borrow P, Rehwinkel J (2015) Viruses transfer the antiviral second messenger cGAMP between cells. *Science* 349: 1228–1232
- Burdette DL, Monroe KM, Sotelo-Troha K, Iwig JS, Eckert B, Hyodo M, Hayakawa Y, Vance RE (2011) STING is a direct innate immune sensor of cyclic di-GMP. *Nature* 478: 515–518
- Cai X, Chiu YH, Chen ZJ (2014) The cGAS-cGAMP-STING pathway of cytosolic DNA sensing and signaling. *Mol Cell* 54: 289–296
- Caly L, Druce J, Roberts J, Bond K, Tran T, Kostecki R, Yoga Y, Naughton W, Tairaoa G, Seemann T et al (2020) Isolation and rapid sharing of the 2019 novel coronavirus (SARS-CoV-2) from the first patient diagnosed with COVID-19 in Australia. *Med J Aust* 212: 459–462
- Carozza JA, Böhnert V, Nguyen KC, Skariah G, Shaw KE, Brown JA, Rafat M, von Eyben R, Graves EE, Glenn JS et al (2020) Extracellular cGAMP is a cancer-cell-produced immunotransmitter involved in radiation-induced anticancer immunity. *Nature Cancer* 1: 184–196
- Chen N, Gallovic MD, Tiet P, Ting JP, Ainslie KM, Bachelder EM (2018) Investigation of tunable acetalated dextran microparticle platform to optimize M2e-based influenza vaccine efficacy. *J Control Release* 289: 114–124
- Coffman RL, Sher A, Seder RA (2010) Vaccine adjuvants: putting innate immunity to work. *Immunity* 33: 492–503
- Corrales L, Glickman L, McWhirter S, Kanne D, Sivick K, Katibah G, Woo S-R, Lemmens E, Banda T, Leong J et al (2015) Direct activation of STING in the tumor microenvironment leads to potent and systemic tumor regression and immunity. *Cell Rep* 11: 1018–1030
- Crotty S (2019) T follicular helper cell biology: a decade of discovery and diseases. *Immunity* 50: 1132–1148
- Cucak H, Yrlid U, Reizis B, Kalinke U, Johansson-Lindbom B (2009) Type I interferon signaling in dendritic cells stimulates the development of lymph-node-resident T follicular helper cells. *Immunity* 31: 491–501
- Cyster JG, Allen CDC (2019) B cell responses: cell interaction dynamics and decisions. *Cell* 177: 524–540
- Demaria O, De Gassart A, Coso S, Gesteremann N, Di Domizio J, Flatz L, Gaide O, Michielin O, Hwu P, Petrova TV et al (2015) STING activation of tumor endothelial cells initiates spontaneous and therapeutic antitumor immunity. *Proc Natl Acad Sci USA* 112: 15408–15413
- Deml L, Speth C, Dierich MP, Wolf H, Wagner R (2005) Recombinant HIV-1 Pr55gag virus-like particles: potent stimulators of innate and acquired immune responses. *Mol Immunol* 42: 259–277
- Diner EJ, Burdette DL, Wilson SC, Monroe KM, Kellenberger CA, Hyodo M, Hayakawa Y, Hammond MC, Vance RE (2013) The innate immune DNA sensor cGAS produces a noncanonical cyclic dinucleotide that activates human STING. *Cell Rep* 3: 1355–1361
- Dubensky Jr TW, Kanne DB, Leong ML (2013) Rationale, progress and development of vaccines utilizing STING-activating cyclic dinucleotide adjuvants. *Ther Adv Vaccines* 1: 131–143
- Ebensen T, Libanova R, Schulze K, Yevs T, Morr M, Guzman CA (2011) Bis-(3',5')-cyclic dimeric adenosine monophosphate: strong Th1/Th2/Th17 promoting mucosal adjuvant. *Vaccine* 29: 5210–5220
- Finkelshtein D, Werman A, Novick D, Barak S, Rubinstein M (2013) LDL receptor and its family members serve as the cellular receptors for vesicular stomatitis virus. *Proc Natl Acad Sci USA* 110: 7306–7311
- Gao Pu, Ascano M, Wu Y, Barchet W, Gaffney B, Zillinger T, Serganov A, Liu Y, Jones R, Hartmann G et al (2013) Cyclic [G(2',5')pA(3',5')p] is the metazoan second messenger produced by DNA-activated cyclic GMP-AMP synthase. *Cell* 153: 1094–1107
- Gentili M, Kowal J, Tkach M, Satoh T, Lahaye X, Conrad C, Boyron M, Lombard B, Durand S, Kroemer G et al (2015) Transmission of innate immune signaling by packaging of cGAMP in viral particles. *Science* 349: 1232–1236
- Gutjahr A, Papagno L, Nicoli F, Kanuma T, Kuse N, Cabral-Piccin MP, Rochereau N, Gostick E, Lioux T, Perouzel E et al (2019) The STING ligand cGAMP potentiates the efficacy of vaccine-induced CD8+ T cells. *JCI Insight* 4: e125107
- Hansen SG, Ford JC, Lewis MS, Ventura AB, Hughes CM, Coyne-Johnson L, Whizin N, Oswald K, Shoemaker R, Swanson T et al (2011) Profound early control of highly pathogenic SIV by an effector memory T-cell vaccine. *Nature* 473: 523–527
- Hanson MC, Crespo MP, Abraham W, Moynihan KD, Szeto GL, Chen SH, Melo MB, Mueller S, Irvine DJ (2015) Nanoparticulate STING agonists are potent lymph node-targeted vaccine adjuvants. *J Clin Invest* 125: 2532–2546
- Hastie E, Cataldi M, Marriott I, Grdzlishvili VZ (2013) Understanding and altering cell tropism of vesicular stomatitis virus. *Virus Res* 176: 16–32
- Hoffmann M, Kleine-Weber H, Pohlmann S (2020) A multibasic cleavage site in the spike protein of SARS-CoV-2 is essential for infection of human lung cells. *Mol Cell* 78: 779–784.e5
- Holecck SA, McAfee MS, Nieves LM, Guzman VP, Manhas K, Fouts T, Bagley K, Blattman JN (2016) Retinaldehyde dehydrogenase 2 as a molecular adjuvant for enhancement of mucosal immunity during DNA vaccination. *Vaccine* 34: 5629–5635
- Hong S, Zhang Z, Liu H, Tian M, Zhu X, Zhang Z, Wang W, Zhou X, Zhang F, Ge Q et al (2018) B cells are the dominant antigen-presenting cells that activate naive CD4(+) T cells upon immunization with a virus-derived nanoparticle antigen. *Immunity* 49: 695–708.e4
- Huang KA, Tan TK, Chen TH, Huang CG, Harvey R, Hussain S, Chen CP, Harding A, Gilbert-Jaramillo J, Liu X et al (2021) Breadth and function of antibody response to acute SARS-CoV-2 infection in humans. *PLoS Pathog* 17: e1009352
- Itano AA, Jenkins MK (2003) Antigen presentation to naive CD4 T cells in the lymph node. *Nat Immunol* 4: 733–739
- Jin L, Hill KK, Filak H, Mogan J, Knowles H, Zhang B, Perraud AL, Cambier JC, Lenz LL (2011) MPYS is required for IFN response factor 3 activation and type I IFN production in the response of cultured phagocytes to bacterial second messengers cyclic-di-AMP and cyclic-di-GMP. *J Immunol* 187: 2595–2601
- Joffre O, Nolte MA, Sporri R, Reis e Sousa C (2009) Inflammatory signals in dendritic cell activation and the induction of adaptive immunity. *Immunol Rev* 227: 234–247
- Junkins RD, Gallovic MD, Johnson BM, Collier MA, Watkins-Schulz R, Cheng N, David CN, McGee CE, Sempowski GD, Shterev I et al (2018) A robust microparticle platform for a STING-targeted adjuvant that enhances both humoral and cellular immunity during vaccination. *J Control Release* 270: 1–13
- Karacostas V, Nagashima K, Gonda MA, Moss B (1989) Human immunodeficiency virus-like particles produced by a vaccinia virus expression vector. *Proc Natl Acad Sci USA* 86: 8964–8967
- Krammer F (2019) The human antibody response to influenza A virus infection and vaccination. *Nat Rev Immunol* 19: 383–397
- Kuse N, Sun X, Akahoshi T, Lissina A, Yamamoto T, Appay V, Takiguchi M (2019) Priming of HIV-1-specific CD8(+) T cells with strong functional properties from naive T cells. *EBioMedicine* 42: 109–119
- Lee E, Jang HE, Kang YY, Kim J, Ahn JH, Mok H (2016) Submicron-sized hydrogels incorporating cyclic dinucleotides for selective delivery and elevated cytokine release in macrophages. *Acta Biomater* 29: 271–281

- Li L, Yin Q, Kuss P, Maliga Z, Millan JL, Wu H, Mitchison TJ (2014) Hydrolysis of 2'3'-cGAMP by ENPP1 and design of nonhydrolyzable analogs. *Nat Chem Biol* 10: 1043–1048
- Li T, Cheng H, Yuan H, Xu Q, Shu C, Zhang Y, Xu P, Tan J, Rui Y, Li P et al (2016) Antitumor activity of cGAMP via stimulation of cGAS-cGAMP-STING-IRF3 mediated innate immune response. *Sci Rep* 6: 19049
- Li XD, Wu J, Gao D, Wang H, Sun L, Chen ZJ (2013) Pivotal roles of cGAS-cGAMP signaling in antiviral defense and immune adjuvant effects. *Science* 341: 1390–1394
- Linterman MA, Hill DL (2016) Can follicular helper T cells be targeted to improve vaccine efficacy? *F1000Res* 5: 88
- Liu Y, Chen S, Pan B, Guan Z, Yang Z, Duan L, Cai H (2016) A subunit vaccine based on rH-NS induces protection against Mycobacterium tuberculosis infection by inducing the Th1 immune response and activating macrophages. *Acta Biochim Biophys Sin* 48: 909–922
- Luo J, Liu XP, Xiong FF, Gao FX, Yi YL, Zhang M, Chen Z, Tan WS (2019) Enhancing immune response and heterosubtypic protection ability of inactivated H7N9 vaccine by using STING agonist as a mucosal adjuvant. *Front Immunol* 10: 2274
- Matrosovich M, Matrosovich T, Carr J, Roberts NA, Klenk HD (2003) Overexpression of the alpha-2,6-sialyltransferase in MDCK cells increases influenza virus sensitivity to neuraminidase inhibitors. *J Virol* 77: 8418–8425
- Mayer A, Maelfait J, Bridgeman A, Rehwinkel J (2017) Purification of cyclic GMP-AMP from viruses and measurement of its activity in cell culture. *Methods Mol Biol* 1656: 143–152
- Merten OW, Hebben M, Bovolenta C (2016) Production of lentiviral vectors. *Mol Ther Methods Clin Dev* 3: 16017
- Milone MC, O'Doherty U (2018) Clinical use of lentiviral vectors. *Leukemia* 32: 1529–1541
- Mohsen MO, Gomes AC, Cabral-Miranda G, Krueger CC, Leoratti FM, Stein JV, Bachmann MF (2017) Delivering adjuvants and antigens in separate nanoparticles eliminates the need of physical linkage for effective vaccination. *J Control Release* 251: 92–100
- Nielsen M, Andreatta M (2016) NetMHCpan-3.0; improved prediction of binding to MHC class I molecules integrating information from multiple receptor and peptide length datasets. *Genome Med* 8: 33
- Nurieva RI, Chung Y, Martinez GJ, Yang XO, Tanaka S, Matskevitch TD, Wang YH, Dong C (2009) Bcl6 mediates the development of T follicular helper cells. *Science* 325: 1001–1005
- O'Garra A (1998) Cytokines induce the development of functionally heterogeneous T helper cell subsets. *Immunity* 8: 275–283
- Ott G, Barchfeld GL, Chernoff D, Radhakrishnan R, van Hoogevest P, Van Nest G (1995) MF59. Design and evaluation of a safe and potent adjuvant for human vaccines. *Pharm Biotechnol* 6: 277–296
- Panagioti E, Klenerman P, Lee LN, van der Burg SH, Arens R (2018) Features of effective T cell-inducing vaccines against chronic viral infections. *Front Immunol* 9: 276
- Pelegri M, Naranjo-Gomez M, Piechaczyk M (2015) Antiviral monoclonal antibodies: can they be more than simple neutralizing agents? *Trends Microbiol* 23: 653–665
- Pichlmair A, Diebold SS, Gschmeissner S, Takeuchi Y, Ikeda Y, Collins MK, Reis e Sousa C (2007) Tubulovesicular structures within vesicular stomatitis virus G protein-pseudotyped lentiviral vector preparations carry DNA and stimulate antiviral responses via Toll-like receptor 9. *J Virol* 81: 539–547
- Powell TJ, Silk JD, Sharps J, Fodor E, Townsend AR (2012) Pseudotyped influenza A virus as a vaccine for the induction of heterotypic immunity. *J Virol* 86: 13397–13406
- Rappuoli R, Mandl CW, Black S, De Gregorio E (2011) Vaccines for the twenty-first century society. *Nat Rev Immunol* 11: 865–872
- Reed LJ, Muench H (1938) A simple method of estimating fifty per cent endpoints. *Am J Epidemiol* 27: 493–497
- Riteau N, Radtke AJ, Shenderov K, Mittereder L, Oland SD, Hieny S, Jankovic D, Sher A (2016) Water-in-oil-only adjuvants selectively promote T follicular helper cell polarization through a type I IFN and IL-6-dependent pathway. *J Immunol* 197: 3884–3893
- Sage PT, Francisco LM, Carman CV, Sharpe AH (2013) The receptor PD-1 controls follicular regulatory T cells in the lymph nodes and blood. *Nat Immunol* 14: 152–161
- Shi S, Zhu H, Xia X, Liang Z, Ma X, Sun B (2019) Vaccine adjuvants: Understanding the structure and mechanism of adjuvanticity. *Vaccine* 37: 3167–3178
- Sun L, Wu J, Du F, Chen X, Chen ZJ (2013) Cyclic GMP-AMP synthase is a cytosolic DNA sensor that activates the type I interferon pathway. *Science* 339: 786–791
- Takaki H, Takashima K, Oshiumi H, Ainai A, Suzuki T, Hasegawa H, Matsumoto M, Seya T (2017) cGAMP promotes germinal center formation and production of IgA in nasal-associated lymphoid tissue. *Med Sci* 5: 35
- Temizoz B, Kuroda E, Ohata K, Jounai N, Ozasa K, Kobiyama K, Aoshi T, Ishii KJ (2015) TLR9 and STING agonists synergistically induce innate and adaptive type-II IFN. *Eur J Immunol* 45: 1159–1169
- Temizoz B, Kuroda E, Ishii KJ (2018) Combination and inducible adjuvants targeting nucleic acid sensors. *Curr Opin Pharmacol* 41: 104–113
- Trumpfheller C, Finke JS, Loópez CB, Moran TM, Moltedo B, Soares H, Huang Y, Schlesinger SJ, Park CG, Nussenzweig MC et al (2006) Intensified and protective CD4+ T cell immunity in mice with anti-dendritic cell HIV gag fusion antibody vaccine. *J Exp Med* 203: 607–617
- Vassilieva EV, Taylor DW, Compans RW (2019) Combination of STING pathway agonist with saponin is an effective adjuvant in immunosenescent mice. *Front Immunol* 10: 3006
- Wang H, Hu S, Chen X, Shi H, Chen C, Sun L, Chen ZJ (2017) cGAS is essential for the antitumor effect of immune checkpoint blockade. *Proc Natl Acad Sci USA* 114: 1637–1642
- Wang J, Li P, Wu MX (2016) Natural STING agonist as an "Ideal" adjuvant for cutaneous vaccination. *J Invest Dermatol* 136: 2183–2191
- Wang J, Li P, Yu Y, Fu Y, Jiang H, Lu M, Sun Z, Jiang S, Lu L, Wu MX (2020) Pulmonary surfactant-biomimetic nanoparticles potentiate heterosubtypic influenza immunity. *Science* 367: eaau0810
- Winter G, Fields S, Brownlee GG (1981) Nucleotide sequence of the haemagglutinin gene of a human influenza virus H1 subtype. *Nature* 292: 72–75
- Wu J, Sun L, Chen X, Du F, Shi H, Chen C, Chen ZJ (2013) Cyclic GMP-AMP is an endogenous second messenger in innate immune signaling by cytosolic DNA. *Science* 339: 826–830
- Xiao JH, Rijal P, Schimanski L, Tharkeshwar AK, Wright E, Annaert W, Townsend A (2018) Characterization of influenza virus pseudotyped with ebolavirus glycoprotein. *J Virol* 92: e00941-17
- Xu R, Johnson AJ, Liggitt D, Bevan MJ (2004) Cellular and humoral immunity against vaccinia virus infection of mice. *J Immunol* 172: 6265–6271
- Yang L, Yang H, Rideout K, Cho T, Joo Ki, Ziegler L, Elliot A, Walls A, Yu D, Baltimore D et al (2008) Engineered lentivector targeting of dendritic cells for in vivo immunization. *Nat Biotechnol* 26: 326–334

- Yi G, Brendel VP, Shu C, Li P, Palanathan S, Cheng Kao C (2013) Single nucleotide polymorphisms of human STING can affect innate immune response to cyclic dinucleotides. *PLoS One* 8: e77846
- Zhang X, Shi H, Wu J, Zhang X, Sun L, Chen C, Chen ZJ (2013) Cyclic GMP-AMP containing mixed phosphodiester linkages is an endogenous high-affinity ligand for STING. *Mol Cell* 51: 226–235
- Zhou D, Duyvesteyn HME, Chen C-P, Huang C-G, Chen T-H, Shih S-R, Lin Y-C, Cheng C-Y, Cheng S-H, Huang Y-C et al (2020) Structural basis for the

neutralization of SARS-CoV-2 by an antibody from a convalescent patient. *Nat Struct Mol Biol* 27: 950–958



License: This is an open access article under the terms of the Creative Commons Attribution License, which permits use, distribution and reproduction in any medium, provided the original work is properly cited.